คุณลักษณะและสมบัติการเป็นตัวเร่งปฏิกิริยาของตัวเร่งปฏิกิริยาโคบอลต์บนตัวรองรับเซอร์โคเนีย ที่ถูกปรับปรุงด้วยโบรอนสำหรับปฏิกิริยาไฮโดรจิเนชันของคาร์บอนมอนอกไซด์

นางสาว นิธินาถ ชิตพงศ์

วิทยานิพนธ์นี้เป็นส่วนหนึ่งของการศึกษาตามหลักสูตรปริญญาวิศวกรรมศาสตรมหาบัณฑิต

สาขาวิชาวิศวกรรมเคมี ภาควิชาวิศวกรรมเคมี

คณะวิศวกรรมศาสตร์ จุฬาลงกรณ์มหาวิทยาลัย

ปีการศึกษา 2550

ลิขสิทธิ์ของจุฬาลงกรณ์มหาวิทยาลัย

CHARACTERISTICS AND CATALYTIC PROPERTIES OF BORON-MODIFED ZIRCONIA-SUPPORTED COBALT CATALYST FOR CARBON MONOXIDE HYDROGENATION

Miss Nithinart Chitpong

A Thesis Submitted in Partial Fulfillment of the Requirements
for the Degree of Master of Engineering Program in Chemical Engineering
Department of Chemical Engineering
Faculty of Engineering
Chulalongkorn University
Academic Year 2007
Copyright of Chulalongkorn University

Thesis Title	CHARACTERISTICS AND CATALYTIC PROPERTIES OF BORON-MODIFED ZIRCONIA-SUPPORTED COBALT CATALYST FOR CARBON MONOXIDE HYDROGENATION
By	Miss Nithinart Chitpong
Field of Study	Chemical Engineering
Thesis Advisor	Assistant Professor Bunjerd Jongsomjit, Ph.D

Accepted by the Faculty of Engineering, Chulalongkorn University in Partial Fulfillment of the Requirements for the Master's Degree

.....Dean of the Faculty of Engineering
(Professor Direk Lavansiri, Ph.D.)

THESIS COMMITTEE

..... Chairman
(Associate Professor Supakanok Thongyai, Ph.D.)

..... Thesis Advisor
(Assistant Professor Bunjerd Jongsomjit, Ph.D.)

..... Member
(Assistant Professor Joongjai Panpranot, Ph.D.)

..... Member
(Assistant Professor Muenduen Phisalaphong, Ph.D.)

..... Member
(Assistant Professor Okorn Mekasuwandumrong, Ph.D.)

นิธินาถ ชิตพงศ์ : คุณลักษณะและสมบัติการเป็นตัวเร่งปฏิกิริยาของตัวเร่งปฏิกิริยาโคบอลต์บนตัวรองรับเซอร์โคเนียที่ถูกปรับปรุงด้วยโบรอนสำหรับปฏิกิริยาไฮโดรจิเนชันของคาร์บอนมอนอกไซด์ (CHARACTERISTICS AND CATALYTIC PROPERTIES OF BORON-MODIFED ZIRCONIA-SUPPORTED COBALT CATALYST FOR CARBON MONOXIDE HYDROGENATION)
อ. ที่ปรึกษา : ผศ. ดร. บรรเจิด จงสมจิตร, 67 หน้า

วิทยานิพนธ์นี้ศึกษาถึงคุณลักษณะและความว่องไวในการเร่งปฏิกิริยาไฮโดรจิเนชันของคาร์บอนมอนอกไซด์ของตัวเร่งปฏิกิริยาโคบอลต์ที่กระจายตัวอยู่บนตัวรองรับเซอร์โคเนียที่ถูกปรับปรุงด้วยโบรอน หลังจากนั้นนำไปฝังเคลือบด้วยโคบอลต์ หลังจากการเผาในอากาศตัวอย่างต่างๆจะถูกนำไปตรวจสอบคุณลักษณะโดยใช้การกระเจิงรังสีเอ็กซ์ การส่องผ่านด้วยกล้องจุลทรรศน์อิเล็กตรอน/ การวัดการกระจายตัวของโลหะ การส่องกราดด้วยกล้องจุลทรรศน์อิเล็กตรอน การรีดักชันแบบโปรแกรมอุณหภูมิและการดูดซับด้วยไฮโดรเจน ปฏิกิริยาไฮโดรจิเนชันของคาร์บอนมอนอกไซด์ (มีอัตราส่วนของไฮโดรเจนต่อคาร์บอนมอนอกไซด์ = 10/1) ถูกใช้เพื่อทดสอบความว่องไวของตัวเร่งปฏิกิริยาและการเลือกเกิดของผลิตภัณฑ์ จากงานวิจัยนั้นพบว่าเซอร์โคเนียที่ถูกปรับปรุงด้วยโบรอนสามารถเพิ่มความว่องไวของตัวเร่งปฏิกิริยาโคบอลต์(ร้อยละ 20 โดยน้ำหนัก) ในปฏิกิริยาไฮโดรจิเนชันของคาร์บอนมอนอกไซด์ ปริมาณของโบรอนที่ใช้ปรับปรุงตัวรองรับเซอร์โคเนียอยู่ในช่วงร้อยละ 0.5 ถึง 3 โดยน้ำหนัก การเพิ่มความว่องไวในการเร่งปฏิกิริยาคือการเพิ่มปริมาณของโลหะโคลอลต์บนพื้นผิวสำหรับการเร่งปฏิริยา โดยการปรับปรุงด้วยโบรอนให้ผลลัพท์คือ (1) ป้องกันการเกิดโคบอลต์ออกไซด์, และ (2) เพิ่มการกระจายตัวของโคบอลต์ออกไซด์ นำไปสู่ความวสามารถในการรีดิวซ์ของโคบอลต์ออกไซด์ไปสู่โลหะโคบอลต์บนพื้นผิว ยิ่งไปกว่านั้นยังพบว่ามันลดการเลือกเกิดผลิตภัณฑ์ของ C_2-C_4 สำหรับการใช้โลหะโคบอลต์ในปริมาณที่ต่างกัน (ร้อยละ 5 ถึง 20 โดยน้ำหนัก) บนตัวรองรับเซอร์โคเนียที่ถูกปรับปรุงด้วยโบรอนในปริมาณร้อยละ 1 โดยน้ำหนักถูกพบว่า ลดความว่องไวของการเร่งปฏิกิริยาเมื่อลดปริมาณของโคลอลต์ แต่จะเพิ่มการเลือกเกิดผลิตภัณฑ์ของ C_2-C_4

ภาควิชา.....วิศวกรรมเคมี..... ลายมือชื่อนิสิต.....นิธินาถ ชิตพงศ์.....
สาขาวิชา.....วิศวกรรมเคมี..... ลายมือชื่ออาจารย์ที่ปรึกษา.....
ปีการศึกษา.....2550.....

##4870346521: MAJOR CHEMICAL ENGINEERING
KEY WORD: ZIRCONIA/ COBALT CATLYST/ BORON MODIFICATION/ CO HYDROGENATION

NITHINART CHITPONG: CHARACTERISTICS AND CATALYTIC PROPERTIES OF BORON-MODIFED ZIRCONIA-SUPPORTED COBALT CATALYST FOR CARBON MONOXIDE HYDROGENATION.
THESIS ADVISOR: BUNJERD JONGSOMJIT, Ph.D., 67 pp.

In the present study, differences in characteristics and catalytic activity towards CO hydrogenation of Co catalysts dispersed on the various B modification on zirconia supports were investigated. After calcination, the various samples were characterized using XRD, SEM/EDX, TEM, TPR and H_2 chemisorption. CO hydrogenation (H_2/CO = 10/1) was also performed to determine the overall activity and selectivity. The B modification on zirconia supports was found to increase the catalytic activities of Co catalyst (20 wt%) during CO hydrogenation. The amounts of B loading in the zirconia support were in the range of 0.5 to 3 wt%. The increased activities were attributed to the larger number of reduced Co metal surface atoms for catalyzing the reaction. It is worth noting that B modification can result in (i) preventing the agglomeration of Co oxide species, and (ii) increasing the dispersion of Co oxide species leading to facilitating the reduction of Co oxide species into Co metal surface atoms. In addition, only a slight decrease in C_2-C_4 selectivity was observed. For the various cobalt loading (5 to 20 wt%) on the 1 wt % of boron modification on zirconia, it was found to decrease the catalytic activity with decreasing the amount of cobalt loading, but an increase in C_2-C_4 selectivity was observed.

Department.....Chemical Engineering... Student's signature...Nithinart...Chitpong
Field of study...Chemical Engineering... Advisor's signature.....
Academic year.....2007.....

ACKNOWLEDGEMENTS

The author would like to express her greatest gratitude and appreciation to her advisor, Dr. Bunjerd Jongsomjit for his invaluable guidance, providing value suggestions and his kind supervision throughout this study. In addition, she is also grateful to Associate Professor Dr. Supakanok Thongyai, as the chairman, Dr. Muenduen Phisalaphong and Dr. Joongjai Panpranot, as the members of the thesis committee. The financial supports from the Thailand Research Fund (TRF) for RMU50-B. and the graduate school at Chulalongkorn University (90^{th} Anniversary of CU under the Golden Jubilee Fund).

Many thanks for kind suggestions and useful help to Miss Sujittra Kittiruangrayub, Mr. Pimchanok Tupabut, many friends both in the petrochemical laboratory and other laboratories who always provide the encouragement and co-operate along the thesis study.

Most of all, the author would like to express her greatest gratitude to her parents and her family who always pay attention to her all the times for suggestions, support and encouragement.

CONTENTS

page

ABSTRACT (IN THAI)……..... iv

ABSTRACT (IN ENGLISH)……... v

ACKNOWLEDGMENTS…… vi

CONTENTS……. vii

LIST OF TABLES……... ix

LIST OF FIGURES…….. x

CHAPTER

I INTRODUCTION…… 1

II LITERATER REVIEWS…….. 3

2.1 Zirconia supported cobalt catalysts…..……..... 3

2.2 Boron modified zirconia supported cobalt catalyst…….. 5

2.3 The other modified zirconia supported cobalt catalyst…… 9

III THEORY…….. 10

3.1 Fischer-Tropsch synthesis (FTS) ……...……..... 10

3.2 Cobalt……... 12

3.2.1 General……..……. 12

3.2.2 Physical properties……....……. 12

3.2.3 Cobalt oxides……....…….…. 15

3.3 Cobalt-based catalysts…….……. 15

3.4 Cobalt-support compound formation (Co-SCF)…….….. 16

3.5 zirconia ……...……..……...……..... 16

3.5.1General feature of zirconia…….. 16

IV EXPERIMENTS……. 19

4.1 Catalyst preparation…….……..... 19

4.1.1 Chemicals……....…….…. 19

4.1.2 Preparation of boron modified zirconia……..….... 19

4.1.3 Preparation of the supported Co samples……... 20

4.1.4 Sample Nomenclature ……...……....…….…. 20

4.2 Catalyst characterization……..……..... 20

4.2.1 N_2 physisorption……. 20

CHAPTER		Page
	4.2.2 X-ray diffraction (XRD)……	21
	4.2.3 Temperature programmed reduction (TPR)……..	21
	4.2.4 Electron microscopy.…….	22
	4.2.5 Transmission Electron Microscopy (TEM)……	22
	4.2.6 Hydrogen chemisorption ……..……	22
	4.3 Reaction study in CO hydrogenation……..	23
	4.3.1 Materials……..…..……	23
	4.3.2 Apparatus…….……..…..……	23
	4.3.3 Procedures.……...…...……..	25
	RESEARCH METHODOLOGY…….….	27
V	RESULTS AND DISCUSSION ……...…...……...……...	28
	5.1 Various boron loading of 20 wt% cobalt on boron modified zirconia supported catalyst…….	28
	5.2 Various Co loading of 1 wt% boron modified zirconia supported catalyst……	41
VI	CONCLUSIONS AND RECOMMENDATIONS……..….	51
	6.1 Conclusions……...…....	51
	6.2 Recommendations……...….	52
REFERENCES…….		53
APPENDICES……..……		56
APPENDIX A: CALCULATION FOR CATALYST PREPARATION…….....		57
APPENDIX B: CALCULATION FOR TOTAL H_2 CHEMISORPTION AND DISPERSION…….…….		58
APPENDIX C: CALIBRATION CURVES.…….……...		59
APPENDIX D: CALCULATION OF CO CONVERSION, REACTION RATE AND SELECTIVITY…….……..……..		62
APPENDIX E: LIST OF PUBICATIONS.……..		63
VITAE …….		67

LIST OF TABLES

Figure page

3.1 Physical properties of cobalt ……..... 13
3.2 Physical properties of zirconia……. 16
3.3 Crystal system of zirconia…… 17
4.1 Chemicals used in the preparation of catalysts……...……. 19
4.2 Operating condition for gas chromatograph……... 24
5.1 BET surface area measurement of 20 wt% cobalt on boron modified supported cobalt catalyst……. 29
5.2 Reduction temperature of catalyst samples (Part I)……. 38
5.3 Results of H_2 chemisorption and selectivity to products (Part I)…..…….. 40
5.4 BET surface area measurement of various cobalt on 1wt% of boron modified supported cobalt catalyst…….. 41
5.5 Reduction temperature of catalyst samples (Part II)…… 48
5.6 Results of H_2 chemisorption and selectivity to products (Part II)…..……. 50
C.1 Conditions use in Shimadzu modal GC-8A and GC-14B……... 59

LIST OF FIGURES

Figure page

3.1 The unit cells of the crystal systems……..…….... 18

3.2 Crystal structure of cubic, tetragonal and monoclinic zirconia…… 18

4.1 Flow diagram of CO hydrogenation system.……...… 26

5.1 Pore size distribution of supports……. 29

5.2 XRD patterns for different ZrO_2 supports consisting of various amounts of boron loading ……. 30

5.3 XRD patterns for different Co/ZrO_2 catalysts with various amounts of boron modification on zirconia support …..... 31

5.4 A typical SEM micrograph and EDX mapping for 20-Co/ZrB-0 sample …… 32

5.5 A typical SEM micrograph and EDX mapping for 20-Co/ZrB-0.5 sample…. 33

5.6 A typical SEM micrograph and EDX mapping for 20-Co/ZrB-1 sample…… 34

5.7 A typical SEM micrograph and EDX mapping for 20-Co/ZrB-3 sample…… 35

5.8 TEM micrographs for different ZrO_2 supports consisting of various amounts of boron loading…… 36

5.9 TEM micrographs for different Co/ZrO_2 catalysts with various amounts of boron modification on zirconia support…… 37

5.10 TPR profiles for different Co/ZrO_2 catalysts with various amounts of boron modification on zirconia support…… 39

5.11 XRD patterns of the 1 wt% of boron modified-supported Co catalyst…….. 42

5.12 A typical SEM micrograph and EDX mapping for 5-Co/ZrB-1 sample…… 43

5.13 A typical SEM micrograph and EDX mapping for 10-Co/ZrB-1 sample…. 44

5.14 A typical SEM micrograph and EDX mapping for 15-Co/ZrB-1 sample…. 45

5.15 A typical SEM micrograph and EDX mapping for 20-Co/ZrB-1 sample…. 46

5.16 TEM micrographs for different Co/ZrO_2 catalysts with various amounts of Co loading on 1 wt% of boron modified supported Co catalysts…….. 47

5.17 TPR profiles for the 1 wt% of boron modified-supported Co catalyst……. 49

C.1 The calibration curve of methane……. 60

C.2 The calibration curve of ethylene……. 60

C.3 The chromatograms of catalyst sample from thermal conductivity detector, gas chromatography Shimadzu model 8A (Molecular sieve 5A column)….. 61

Figure page

C.4 The chromatograms of catalyst sample from flame ionization detector, gas chromatography Shimadzu model 14B (VZ10 column)……..... 61

CHAPTER I

INTRODUCTION

In general, a supported catalyst usually consists of three components; (i) a catalytic phase, (ii) a promoter, and (iii) a support or carrier. As known, the catalytic properties apparently depend on the components as mentioned above. The catalytic phase can be metals, metal oxides and so on. It can be employed under a specified catalytic reaction. It is known that the catalytic performance is usually elevated using a promoter such as a noble metal. Besides the catalytic phase and promoter, it should be mentioned that a support could play a crucial role based on the catalytic performance. Basically, a support material acts as a carrier for the catalytic phase to be well dispersed on it. However, due to the supporting effect along with dispersion of the catalytic phase, the properties of a catalyst could be altered with various supports used. It is reported that many inorganic supports such as silica (SiO_2), alumina (Al_2O_3), titania (TiO_2), zirconia (ZrO_2) , and zeolites (R.C. Reuel and C.H. Bartholomew, 1984; M. Kraum and M. Baerns,1999; G. Jacobs *et al.,* 2002; N.N. Madikizela and N.J. Coville, 2002; D.I. Enache et al. 2004) have been extensively studied for years. During the part decades, zirconia-supported cobalt catalysts have been investigated by many authors. However, it should be noted that the properties of zirconia itself may not be suitable as a sole support for the supported cobalt catalyst. Hence, the modification of the zirconia support would be necessary. It has been reported that some metals such as boron were used to modify the properties of other supports such as alumina or titania. (M.A. Stranick *et al*., 1986; J. Li and N.J. Coville , 1999,2001; N.J. Coville and J. Li, 2002) I showed a significant enhancement of catalytic activity of cobalt due to in creased cobalt dispersion.

In the present study, the effect of boron modification of zirconia on the characteristics and catalytics properties of zirconia-supported cobalt catalyst during CO hydrogenation was investigated. The study was scoped as follows:

1. Preparation of boron modified zirconia supports (0, 0.5, 1 and 3 wt%B) by impregnation method.

2. Characterization of the boron modified support samples using BET surface area, X-ray diffraction (XRD), scanning electron microscopy (SEM) and energy dispersive X-ray spectroscopy (EDX), and transmission electron spectroscopy (TEM).

3. Preparation of modified zirconia-based supported Co catalyst (5,10 and 20 wt% Co) using the incipient wetness impregnation method.

4. Characterization of the catalyst samples using BET surface area, X-ray diffraction (XRD), temperature programmed reduction (TPR), hydrogen chemisorption, scanning electron microscopy (SEM) and energy dispersive X-ray spectroscopy (EDX) and transmission electron spectroscopy (TEM).

5. Reaction study of the catalyst samples in carbon monoxide (CO) hydrogenation at 220^{o}C and 1 atm and a H_2/CO ratio of 10.

CHAPTER II

LITERATURE REVIEWS

There are several studies of zirconia-supported catalysts. Many researchers have been found better knowledge about zirconia especially supported cobalt catalyst in Fischer-Tropsch synthesis. These reports are very useful and will use to develop works for the future.

2.1 Zirconia supported cobalt catalyst

M. Baerns et al. (1999) The dependence of the activity of cobalt-based catalysts for Fischer–Tropsch synthesis on the type of cobalt precursor and support material was studied. Titania-supported catalysts were prepared by means of incipient wetness impregnation (IW), precipitation (PR) and spreading (SP) techniques. All catalysts were characterised by XRD, XPS, TPR and CO pulse experiments. The catalytic performance of the catalysts was examined at a total pressure of 20 bar, a temperature of 200^{o}C, a space velocity (GHSV) of 1200 h−1and using a syngas having a H2 to CO ratio equal to 2.

For titania-supported catalysts, the use of oxalate, acetate and acetyl acetonate as cobalt precursors resulted in a higher activity compared with the reference catalyst prepared from nitrate. The activities determined can be slightly correlated with an increasing cobalt dispersion, whichwas affected by the preparation procedure and type of precursor. The range of chain growthprobabilities increased in the following order: cobalt(III) acetyl acetonate (α = 0.71)<cobalt acetate (α = 0.74)<cobalt(II)acetyl acetonate, cobalt oxalate, cobalt nitrate, cobalt-EDTA (α = 0.82–0.84). On adding 0.1 wt.% Ru to the catalyst made from cobalt(III) acetyl acetonate, α increased from 0.71 to 0.80.

For catalysts prepared by incipient wetness impregnation, ceria and zirconia were additionally used as supports. The activity changed in the following order: ZrO_2 <TiO_2 <CeO_2. The α-value for ceria-and zirconia-supported cobalt catalysts amounted to 0.81 and 0.69, respectively.

D. I. Enache et al. (2004) studied the activity and the selectivity of cobalt catalysts supported on a crystallized and on an amorphous zirconia were compared with cobalt supported on a γ-alumina catalyst. The catalysts supported on zirconium dioxide were found to present a better reducibility of the active phase and also to be capable of hydrogen adsorption via a spillover mechanism. It is proposed that these properties could account for a better catalytic activity and an increase of the chain growth probability (α). At the same time, the estimated quantity of crystallized Co_3O_4 obtained after airflow calcination (for the same total cobalt loading) is related with the surface area of the support.

J. Panpranot et al. (2005) reported nanocrystalline zirconia have been prepared by the glycothermal method with two different glycols (1,4-butanediol and 1,5-pentanediol) and employed as the support for cobalt catalysts. Commercial zirconia supported cobalt catalyst was also prepared and used as a reference material. The glycothermal-derived zirconia possesses large surface areas with crystallite sizes of 3–4 nm. The catalytic activities for CO hydrogenation of the glycothermal-derived zirconia supported cobalt catalysts were found to be much higher than that of the commercial zirconia supported one. However, the cobalt catalysts supported on zirconia prepared in 1,4-butanediol with lower amount of Zr content in the starting solution exhibited higher activities than the ones supported on zirconia prepared in 1,5-pentanediol. The results suggest that the different crystallization mechanism occurred in the two glycols may affect the amount of crystal defects produced in the corresponding zirconia. As shown by TPR profiles, lower metal-support interaction was observed for the catalysts supported on the zirconia formed via solid-state reaction in 1,4-butanediol (more defects). Consequently, higher active surface cobalt was available for H_2 chemisorption and CO hydrogenation reaction.

J. Panpranot et al. (2006) reported nanocrystalline zirconia was prepared by decomposition of zirconium tetra n-propoxide in 1,4-butanediol and was employed as a support for cobalt catalysts. The activity and the selectivity of the catalysts in CO hydrogenation were compared with cobalt supported on commercial available micron- and nano-sized zirconia. The catalytic activities were found to be in the order: Co/ZrO_2-nano-glycol>>Co/ZrO_2-nano-com > Co/ZrO_2-micron-com. Compared to the

micron-sized zirconia supported one, the use of commercial nano-sized zirconia resulted in higher CO hydrogenation activity but lower selectivity for longer chain hydrocarbons (C_4–C_6), whereas the use of glycothermal-derived nanocrystalline zirconia exhibited both higher activity and selectivity for C_4–C_6. The better performance of the latter catalyst can be ascribed to not only the effect of the crystallite size but also the presence of pure tetragonal phase of zirconia.

2.2 Boron modified zirconia supported cobalt catalyst

M. Stranick et al. (1987) reported the influence of boron on the chemical state and dispersion of Co/Al_2O_3 catalysts has been investigated by bulk and surface spectroscopic techniques. Three series of Co/Al_2O_3catalysts were studied: one containing a constant Co loading of 3 wt% and boron loadings of 0.3 to 3 wt% and two series containing 0.7 to 10 wt% Co and constant boron loadings of either 0 or 3 wt% Co. In the absence of boron. Co dispersion decreased with increasing Co loading above 1.5 wt% Co. The presence of boron had little effect on Co dispersion at low Co loadings, while catalysts with Co loadings in excess of 1.5 wt% exhibited an increase in Co dispersion compared to boron-free catalysts. X-ray photoelectron spectroscopy, diffuse reflectance spectroscopy, and gravimetric analysis were used to quantify the Co species present on the catalysts as a function of both Co and boron loading. In the absence of boron, Co exists as tetrahedral and octahedral Co^{2+} at low Co loadings, while Co_3O_4 is the primary phase at higher Co loadings. In the presence of boron, Co_3O_4 formation is suppressed for catalysts with Co loadings less than 8 wt% in favor of octahedral Co^{2+} and minor amounts of Co borate. The formation of Co_3O_4 occurs at Co loadings greater than 6 wt% for boron-containing catalyst. A mechanism is described to account for the effect of boron on the dispersion and chemical state of Co.

J. Li et al.(1999) reported the effect of boron (as H_3BO_3) on the CO hydrogenation ability of Co/TiO_2 catalysts was investigated using XRD, LRS, TGA, DRIFTS and a fixed bed flow reactor. The introduction of boron (0.02±1.5%) into a 10 wt% Co/TiO_2 catalyst decreased the Co_3O_4 crystallite size (26±16 nm) in the oxidic catalysts (calcined at 300°C) and decreased the hydrogen uptake (0.35±0.9

ml/g cat) in the reduced catalyst. Reduction of the Co/TiO_2 catalyst was made more difficult by the presence of boron. The CO conversion and overall hydrogenation rate decreased with decreasing ease of reducibility and decreasing cobalt dispersion caused by boron. Turnover frequency (ca. $20x10^{-3}$ S^{-1}), however, remained constant throughout and was independent of the extent of reduction and dispersion of the catalysts. This provides further evidence of the structure-insensitivity of supported Co Fischer Tropsch catalysts. Addition of small amounts of B (<0.1%) do, however, result in an increase in α, less CH_4 production and an increase in the olefin/parafin ratio. This suggests an increase in the monomer propagation to termination ratio. At higher B loadings, product selectivity shifted to the lower molecular weight hydrocarbons and CO_2 selectivity increased (0±2.5%).

J. Li et al.(2001) reported TiO_2 was treated with boron (0.05, 0.1%; boric acid source) to give B/TiO_2. $Co(NO_3)_2{\cdot}6H_2O$ (10% Co) was then added to both TiO_2 and B/TiO_2 (incipient wetness) and the materials were then sulfided with 100, 200 and 500 ppm $(NH_4)_2S$. The sulfided Co/TiO_2 catalysts with and without boron were characterised by TPR and O_2 titration and evaluated for Fischer–Tropsch synthesis. Low-level sulfur addition (100, 200 ppm S) did not significantly influence the activity and selectivity of the catalysts. The addition of a higher-level loading of sulfur (500 ppm S) resulted in severe sulfur poisoning of catalysts (80% decrease in reaction rate), but the modification of Co/TiO_2 by boron retarded this poisoning (35% decrease in reaction rate). A shift in the product distribution to light molecular weight hydrocarbons (α U 0.32) was observed for the 500 ppm S loaded catalyst (no boron addition) while boron addition retarded this shift (α U 0.47). The effect of boron on the sulfur poisoning resistance of the Co/TiO_2 catalysts is discussed.

J. Li et al. (2002) studied the effect of the addition of small amounts of boron, ruthenium and rhenium on the Fischer–Tropsch (F–T) catalyst activity and selectivity of a 10wt.% Co/TiO_2 catalyst has been investigated in a continuously stirred tank reactor (CSTR). A wide range of synthesis gas conversions has been obtained by varying space velocities over the catalysts. The addition of a small amount of boron (0.05 wt.%) onto Co/TiO2 does not change the activity of the catalyst at lower space times and slightly increases synthesis gas conversion at higher space times. The

product selectivity is not significantly influenced by boron addition for all space velocities investigated. Ruthenium addition (0.20 wt.%) onto Co/TiO_2 and CoB/TiO_2 catalysts improves the catalyst activity and selectivity. At a space time of 0.5 h-g cat./NL, synthesis gas conversion increases from 50–54 to 68–71% range and methane selectivity decreases from 9.5 to 5.5% (molar carbon basis) for the promoted catalyst. Among the five promoted and non-promoted catalysts, the rhenium promoted Co/TiO_2 catalyst (0.34 wt.% Re) exhibited the highest synthesis gas conversion, and at a space time of 0.5 h-g cat./NL, synthesis gas conversion was 73.4%. In comparison with the results obtained in a fixed bed reactor, the catalysts displayed a higher F–T catalytic activity in the CSTR.

G. Jacobs et al. (2002) Temperature programmed reduction (TPR) and hydrogen chemisorption combined with reoxidation measurements were used to define the reducibility of supported cobalt catalysts. Different supports (e.g. Al_2O_3, TiO_2, SiO_2, and ZrO_2 modified SiO_2 or Al_2O_3) and a variety of promoters, including noble metals and metal cations, were examined. Significant support interactions on the reduction of cobalt oxide species were observed in the order $Al_2O_3 > TiO_2 > SiO_2$. Addition of Ru and Pt exhibited a similar catalytic effect by decreasing the reduction temperature of cobalt oxide species, and for Co species where a significant surface interaction with the support was present, while Re impacted mainly the reduction of Co species interacting with the support. For catalysts reduced at the same temperature, a slight decrease in cluster size was observed in H2 chemisorption/pulse reoxidation with noble metal promotion, indicating that the promoter aided in reducing smaller Co species that interacted with the support. On the other hand, addition of non-reducible metal oxides such as B, La, Zr, and K was found to cause the reduction temperature of Co species to shift to higher temperatures, resulting in a decrease in the percentage reduction. For both Al_2O_3 and SiO_2, modifying the support with Zr was found to enhance the dispersion. Increasing the cobalt loading, and therefore the average Co cluster size, resulted in improvements to the percentage reduction. Finally, a slurry phase impregnation method led to improvements in the reduction profile of Co/Al_2O_3.

N.J. Coville et al.(2002) studied a series of $Co/B/TiO_2$ (B = ammonium borate, boric acid, *o*-carborane, 0.01–1.5 wt.% B) catalysts were synthesized. The addition of

boron decreased the reducibility of the Co as determined from temperature-programmed reduction studies and H2 reduction/O2back titration studies. This in turn decreased the FT activity but not the turnover frequency of the Co catalyst.

Y. Brik et al. (2002) studied cobalt- and cobalt–boron-loaded TiO_2 (anatase) catalysts were prepared and characterized before and after catalytic tests by XRD, HRTEM, IR, UV–visible, and laser Raman spectroscopy. Theiractivity was investigated in oxidative dehydrogenation (ODH) of ethane. In the absence of boron, the best performances were exhibited by the sample containing 7.6 wt% Co, which was selected for further investigations. At 550◦C, it displayed a stationary state with a conversion of 22.2% and an ethylene selectivity around 60%. This catalyst also showed in the first 3 h on stream a 30% decay in activity that was attributed to a concomitant loss of specific surface area and the formation of $CoTiO_3$ and $Co2TiO_4$ phases. The addition of 0.25 wt% boron to this $Co(7.6)/TiO_2$ sample improved the ethane conversion and the ethylene selectivity, which attained 28.4 and 67%, respectively. Boron concentrations superior to 0.25 wt% negatively affected the catalysts performances, probably because at high loadings it profoundly modified the acid–base properties of the surface. XRD and HRTEM analyses showed that at the same time the size of Co_3O_4 crystallites decreased. IR investigations confirmed the increase in acidity upon boron addition and the decrease in strength of the basic sites which were involved in the dehydrogenation processes.

The catalytic behavior and the acid–base properties of $Co(7.6)/TiO_2$ loaded with different amounts of boron were also studied using butan-2-ol conversion. Boron addition enhanced the dehydration and the dehydrogenation reactions. However, above 0.25 wt% it decreased the dehydrogenation activity, confirming the modifications of the properties of the acid–base centers revealed by the IR studies. For this optimal concentration of boron, the activity and the selectivity in butan-2-ol dehydrogenation exhibited a maximum that coincided with the one observed in the ethane ODH, which suggests that both reactions possibly involved the same type of active centers.

2.3 The other modified zirconia supported cobalt catalyst

P. Soisuwan et al. (2006) reported Nanocrystalline zirconia and m-modified zirconia (m = Si and Y) have been prepared by the modified Pechini_s method and employed as supports for cobalt catalysts. Addition of a small amount of Si or Y during the preparation of nanocrystalline zirconia did not alter the average crystallite sizes and BET surface areas of the tetragonal zirconia. However, zirconia primary particles appeared to be more agglomerated when Si/Zr and Y/Zr were greater than 0.005 and 0.01, respectively. The Si- and Y-modified zirconia supported cobalt catalysts with higher m/Zr showed higher H_2 chemisorption and CO hydrogenation activities.

CHAPTER III

THEORY

3.1 Fischer-Tropsch synthesis (FTS)

Fischer-Tropsch synthesis (FTS) or CO hydrogenation reaction, the production of liquid hydrocarbons from synthesis gases (CO and H_2) is a promising, developing route for environmentally sound production of chemicals and fuels from coal and natural gas. During the past decades, FTS has been developed continuously by many researchers, although the rise and fall in research intensity on this process has been highly related to the demands for liquid fuels and relative economics. This synthesis is basically the reductive polymerization (oligomerization) of carbon monoxide by hydrogen to form organic products containing mainly hydrocarbons and some oxygenated products in lesser amounts. The main reactions of FTS are:

$$CO + 3H_2 \rightarrow CH_4 + H_2O \quad (1)$$

$$CO + 2H_2 \rightarrow (\frac{1}{n})(C_nH_{2n}) + H_2O \quad (2)$$

$$CO + H_2O \rightarrow CO_2 + H_2 \quad (3)$$

$$2CO \rightarrow C + CO_2 \quad (4)$$

Equations (1) is the formation of methane, the equation (2) is the synthesis of hydrocarbons higher than methane, the equation (3) is the water-gas shift reaction, and the equation (4) is the Boudouard reaction resulting in which results in deposition of carbon. The reaction mechanism of methanation can be described by the following set of mechanism:

$CO + * = CO*$

$CO* + * = C* + O*$

$H_2 + 2* = 2H*$

$C* + H* = CH* + *$

$CH* + H* = CH_2* + *$

$CH_2* + H* = CH_3* + *$

$CH_3* + H* = CH_4(g) + 2*$

$O* + H* = OH* + *$

$OH* + H* = H_2O(g) + 2*$

Normally, catalysts used for FTS are group VIII metals. By nature, the hydrogenation activity increases in order of Fe < Co < Ni < Ru. Ru is the most active. Ni forms predominantly methane, while Co yields much higher ratios of paraffins to olefins and much less oxygenated products such as alcohols and aldehydes than Fe does.

Commercially, Entrained bed reactors or slurry bubble column reactors are used in FTS since they can remove heat from this exothermic synthesis, allowing better temperature control.

The current main goal in FTS is to obtain high molecular weight, straight chain hydrocarbons. However, methane and other light hydrocarbons are always present as less desirable products from the synthesis. According to the Anderson-Schulz-Flory (ASF) product distribution, typically 10 to 20% of products from the synthesis are usually light hydrocarbon (C_1-C_4). These light alkanes have low boiling points and exist in the gas phase at room temperature, which is inconvenient for transportation. Many attempts have been made to minimize these by-products and increase the yield of long chain liquid hydrocarbons by improving chain growth probability. It would be more efficient to be able to convert these less desirable products into more useful forms, rather than re-reforming them into syngas and recycling them (R.J. Farrauto and C.H. Bartholomew, 1997). Depending upon the type of catalyst used, promoters, reaction conditions (pressure, temperature and H_2/CO ratios), and type of reactors, the distribution of the molecular weight of the hydrocarbon products can be noticeably varied.

3.2 Cobalt (R.S. Young 1960; K. Othmer, 1991)

3.2.1 General

Cobalt, a transition series metallic element having atomic number 27, is similar to silver in appearance.

Cobalt and cobalt compounds have expended from use colorants in glasses and ground coat fits for pottery to drying agents in paints and lacquers, animal and human nutrients, electroplating materials, high temperature alloys, hard facing alloys, high speed tools, magnetic alloys, alloys used for prosthetics, and used in radiology. Cobalt is also as a catalyst for hydrocarbon refining from crude oil for the synthesis of heating fuel.

3.2.2 Physical Properties

The electronic structure of cobalt is [Ar] $3d^7 4s^2$. At room temperature the crystalline structure of the α (or ε) form, is close-packed hexagonal (cph) and lattice parameters are a = 0.2501 nm and c = 0.4066 nm. Above approximately 417°C, a face-centered cubic (fcc) allotrope, the γ (or β) form, having a lattice parameter a = 0.3554 nm, becomes the stable crystalline form

The scale formed on unalloyed cobalt during exposure to air or oxygen at high temperature is double-layered. In the range of 300 to 900°C, the scale consists of a thin layer of mixed cobalt oxide, Co_3O_4, on the outside and cobalt (II) oxide, CoO, layer next to metal. Cobalt (III) oxide, Co_2O_3, may be formed at temperatures below 300°C. Above 900°C, Co_3O_4 decomposes and both layers, although of different appearance, are composed of CoO only. Scales formed below 600°C and above 750°C appear to be stable to cracking on colling, whereas those produced at 600-750°C crack and flake off the surface.

Cobalt forms numerous compounds and complexes of industrial importance. Cobalt, atomic weight 58.933, is one of the first transition series of Group 9 (VIIIB). There are thirteen know isotope, but only three are significant: ^{59}Co is the only stable and naturally occurring isotope; ^{60}Co has a half-life of 5.3 years and is a common source of γ-source for MÖssbauer spectroscopy.

Cobalt exists in the +2 or +3 valance states for the major of its compounds and complexes. A multitude of complexes of the cobalt (III) ion exists, but few stable simple salt are know. Octahedral stereochemistries are the most common for cobalt (II) ion as well as for cobalt (III). Cobalt (II) forms numerous simple compounds and complexes, most of which are octahedral or tetrahedral in nature; cobalt (II) forms more tetrahedral complex than other transition-metal ions. Because of the small stability difference between octahedral and tetrahedral complexes of cobalt (II), both can be found equilibrium for a number of complexes. Typically, octahedral cobalt (II) salts and complexes are pink to brownish red; most of the tetrahedral Co (II) species are blue.

Table 3.1 Physical properties of cobalt (K. Othmer, 1991)

Property	Value
atomic number	27
atomic weight	58.93
transformation temperature, ^{o}C	417
heat of transformation, J/g[a]	251
melting point, ^{o}C	1493
latent heat of fusion, ΔH_{fus} J/g[a]	395
boiling point, , ^{o}C	3100
latent heat of vaporization at bp, ΔH_{vap} kJ/g[a]	6276
specific heat, J/(g·^{o}C)[a]	
15-100^{o}C	0.442
molten metal	0.560
coefficient of thermalexpansion, $^{o}C^{-1}$	
cph at room temperature	12.5
fcc at 417^{o}C	14.2
thermal conductivity at 25 ^{o}C, W/(m·K)	69.16
thermal neutron absorption, Bohr atom	34.8
resistivity, at 20 ^{o}C[b], $10^{-8}\Omega$·m	6.24
Curie temperature, ^{o}C	1121

Table 3.1 Physical properties of cobalt (cont.)

Property		Value	
saturation induction, $4\pi I_s$, T[c]		1.870	
permeability, μ			
initial		68	
max		245	
residual induction, T[c]		0.490	
coercive force, A/m		708	
Young's modulus, Gpac		211	
Poisson's ratio		0.32	
Hardness[f], diamond pyramid, of %Co		99.9	99.98[e]
At 20 °C		225	253
At 300 °C		141	145
At 600 °C		62	43
At 900 °C		22	17
strength of 99.99 %cobalt, MPa[g]	as cast	annealed	sintered
tensile	237	588	679
tensile yield	138	193	302
compressive	841	808	
compressive yield	291	387	

[a] To convert J to cal, divided by 4.184.

[b] conductivity = 27.6 % of International Annealed Copper Standard.

[c] To convert T to gauss, multiply by 10^4.

[d] To convert GPa to psi , multiply by 145,000.

[e] Zone refined.

[f] Vickers.

[g] To convert MPa to psi , multiply by 145.

3.2.3 Cobalt Oxides

Cobalt has three well-know oxides:

Cobalt (II) oxide, CoO, is an olive green, cubic crystalline material. Cobalt (II) oxide is the final product formed when the carbonate or the other oxides are calcined to a sufficiently high temperature, preferably in a neutral or slightly reducing atmosphere. Pure cobalt (II) oxide is a difficult substance to prepare, since it readily takes up oxygen even at room temperature to re-form a higher oxide. Above about 850°C, cobalt (II) oxide form is the stable oxide. The product of commerce is usually dark gray and contains 77-78 wt % cobalt. Cobalt (II) oxide is soluble in water, ammonia solution, and organic solvents, but dissolves in strong mineral acids. It is used in glass decorating and coloring and is a precursor for the production of cobalt chemical.

Cobalt (II) oxide, Co_2O_3, is form when cobalt compounds are heated at a low temperature in the presence of an excess of air. Some authorities told that cobalt (III) oxide exists only in the hydrate form. The lower hydrate may be made as a black power by oxidizing neutral cobalt solutions with substances like sodium hypochlorite. Co_2O_3 or $Co_2O_3.H_2O$ is completely converted to Co_3O_4 at temperatures above 265°C. Co_3O_4 will absorb oxygen in a sufficient quantity to correspond to the higher oxide Co_2O_3.

Cobalt oxide, Co_3O_4, is formed when cobalt compounds, such as the carbonate or the hydrated sesquioxide, are heated in air at temperatures above approximately 265°C and not exceeding 800°C.

3.3 Co-based catalysts

Supported cobalt (Co) catalysts are the preferred catalysts for the synthesis of heavy hydrocarbons from natural gas based syngas (CO and H_2) because of their high Fischer-Tropsch (FT) activity, high selectivity for linear hydrocarbons, and low activity for the water gas shift reaction. It is known that reduced cobalt metal, rather than its oxides or carbides, is the most active phase for CO hydrogenation in such catalysts. Investigations have been done to determine the nature of cobalt species on various supports such as alumina, silica, titania, magnesia, carbon, and zeolites. The influence of various types of cobalt precursors used was also investigated. It was

found that the used of organic precursors such as Co (III) acetyl acetate resulting in an increase of CO conversion compared to that of cobalt nitrate (M. Kraum and M. Baerns, 1999).

3.4 Cobalt-Support Compound Formation (Co-SCF)

Compound formation between cobalt metal and the support can occur under pretreatment and/or reaction conditions, leading to catalyst deactivation. The compound formation of cobalt metal with support materials, however, is difficult to predict because of the lack of sufficient thermodynamic data. Co-support compound formation can be detected evidentially.

3.5 Zirconia

3.5.1 General feature of zirconia

Table 3.2 Physical properties of zirconia

Properties	
Systematic	Zirconium dioxide Zirconium(IV)dioxide
Other names	Zirconia Baddeleyite
Molecular formula	ZrO_2
Molar mass	123.22 g/mol
Appearance	white or colourless solid (when pure)
Density and phase	5.89 g/cm3, solid
Solubility in water	insoluble
Melting point	2715 °C

Zirconia exhibits three polymorphs, the monoclinic, tetragonal, and cubic phases. Figure 2.1 shows the typical systems: cubic, tetragonal and monoclinic ones. Crystal structure of cubic, tetragonal and monoclinic zirconia are shown in Figure 2.2 The monoclinic is stable up to ~1170^{o}C, at which temperature it transforms into the tetragonal phase, which is stable up to 2370^{o}C (Cormak and Parker, 1990). The stabilization of the tetragonal phase below 1100^{o}C is important in the use of zirconia as a catalyst in some reaction. Above 2370^{o}C, the cubic phase is stable and it exists up to the melting point of 2680^{o}C. Due to the martens tic nature of the transformations, neither the high temperature tetragonal nor cubic phase can be quenched in rapid cooling to room temperature. However, at low temperature, a metastable tetragonal zirconia phase is usually observed when zirconia is prepared by certain methods, for example by precipitation from aqueous salt solution or by thermal decomposition of zirconium salts. This is not the expected behavior according to the phase diagram of zirconia (i.e., monoclinic phase is the stable phase at low temperatures). The presence of the tetragonal phase at low temperatures can be attributed to several factors such as chemical effects, (the presence of anionic impurities) (Srinivasan et al., 1990 and Tani et al., 1982) structural similarities between the tetragonal phase and the precursor amorphous phase (Osendi et al., 1985; Tani, 1982 and Livage, 1968) as well as particle size effects based on the lower surface energy in the tetragonal phase compared to the monoclinic phase (Garvie, 1978; Osendi et al., 1985 and Tani 1982). The transformation of the metastable tetragonal form into the monoclinic form is generally complete by 650-700 ^{o}C.

Table 3.3 Crystal systems of zirconia**.**

Crystal system	Unit cell shape
Cubic	$a = b = c$, $\alpha = \beta = \gamma = 90^{o}$
Tetragonal	$a = b \neq c$, $\alpha = \beta = \gamma = 90^{o}$
Monoclinic	$a \neq b \neq c$, $\alpha = \gamma = 90^{o}$, $\beta \neq 90^{o}$

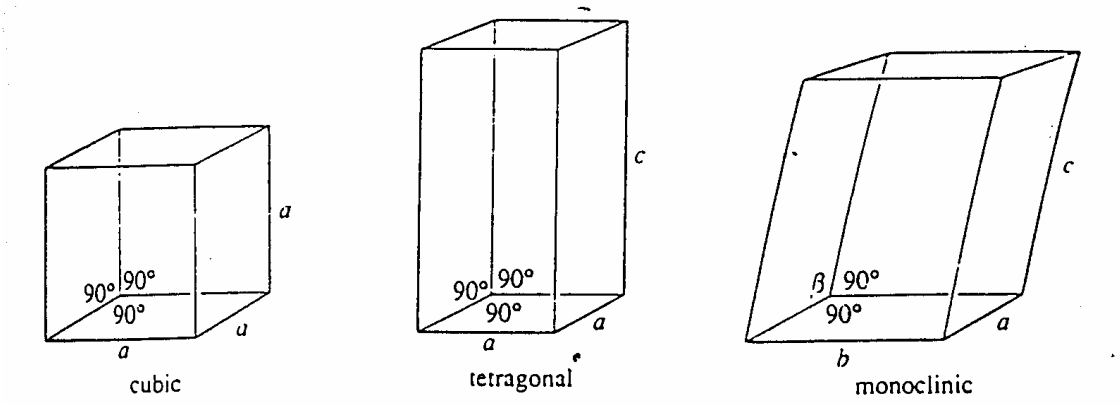

Figure 3.1 The unit cells of the crystal systems. (West, 1997)

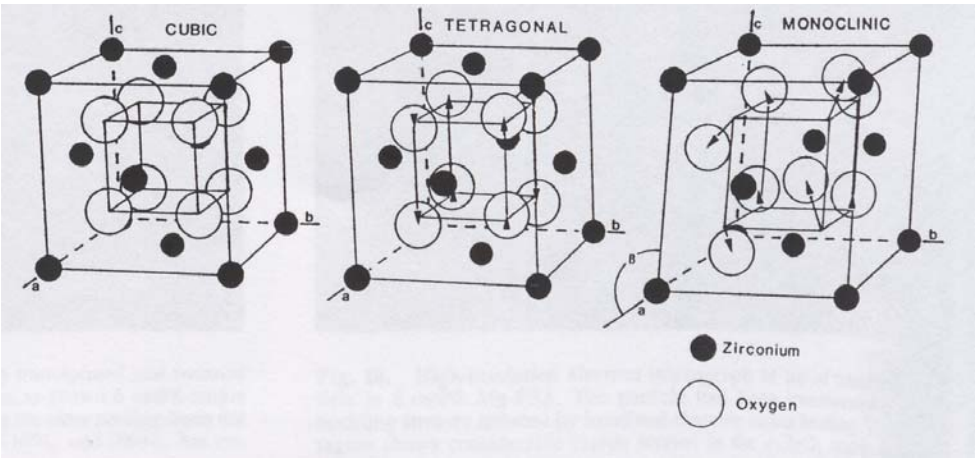

Figure 3.2 Crystal structure of cubic, tetragonal and monoclinic zirconia. (Heuer, 1987)

CHAPTER IV

EXPERIMENTAL

This chapter consists of experimental systems and procedures used in this work which is divided into three parts consisting of catalyst preparation (4.1), catalyst characterization (4.2) and reaction study in CO hydrogenation (4.3).

The samples were prepared and analyzed by means of N_2 physisorption, X-ray diffraction (XRD), scanning electron microscopy (SEM), energy dispersion X-ray spectroscopy (EDX), transmission electron spectroscopy (TEM), and temperature-programmed reduction (TPR). The reaction study was performed in order to measure activity and product selectivity toward CO hydrogenation at 220^{o}C and 1 atm.

4.1 Catalyst preparation

4.1.1 Chemicals

The details of chemicals used in this experiment are shown in Table 4.1

Table 4.1 Chemicals used in the preparation of catalysts.

Chemical	Supplier	CAS. Number	Product Number
Cobalt (II) nitrate exahydrate ($Co(NO_3)_2 \cdot 6H_2O$)	Aldrich	10026-22-9	239267
Boric acid (H_3BO_3)	Aldrich	-	339067
Zirconium dioxide(ZrO_2), micron powder	Aldrich	1314-23-4	230693

4.1.2 Preparation of the boron modified zirconia

The B-modified ZrO_2 supports were prepared by the incipient impregnation method. First, boron was impregnated on the ZrO_2 support [from Aldrich(< 5 micron, 99.99%)] using a solution of boric acid (99.99%, Aldrich) to produce B-modified ZrO_2 supports having 0.5, 1 and 3 wt% of B. Then , the B-modified ZrO_2 supports were calcined at 500^{o}C for 4 h prior to impregnation of cobalt.

4.1.3 Preparation of the supported Co samples

Cobalt nitrate [$Co(NO_3)_2 \cdot 6H_2O$] was dissolved in deionized water and impregnated on the support as derived above to give a final catalyst with 5, 10, 15 and 20 wt% of cobalt. The catalyst precursor was dried at 110^{o}C for 12 h and calcined in air at 500^{o}C for 4 h.

4.1.4 Sample nomenclature

The nomenclature used for the support and catalyst samples in this study is as follows:

ZrB-0 refers to the ZrO_2 support without B modification.

ZrB-*i* refers to the B-modified ZrO_2 having *i* wt% of B.

***a*-Co/support** refers to supported cobalt catalyst on various supports as derived above, where *a* is the weight percents of cobalt.

4.2. Catalyst characterization

4.2.1 N_2 physisorption

BET apparatus for the single point method

The reaction apparatus of BET surface area measurement consisted of two feed lines for helium and nitrogen using a Micrometritics Chemisorb 2750. The flow rate of the gas was adjusted by means of fine-metering valve on the gas chromatograph. The sample cell made from pyrex glass. The mixture gases of helium and nitrogen flowed through the system at the nitrogen relative of 0.3. The catalyst sample (ca. 0.2 to 0.5 g) was placed in the sample cell, which was then heated up to 200 ^{o}C and held at this temperature for 1 h. After the catalyst sample was cooled down to room temperature, nitrogen uptakes were measure as follows.

Step (1) Adsorption step: The sample that set in the sample cell was dipped into liquid nitrogen. Nitrogen gas that flowed through the system was adsorbed on the surface of the sample until equilibrium was reached.

Step (2) Desorption step: The sample cell with nitrogen gas-adsorption catalyst sample dipped into the water at room temperature. The adsorbed nitrogen gas was desorbed from the surface of the sample. This step was completed when the indicator line was in the position of base line.

Step (3) Calibration step: 1 ml of nitrogen gas at atmospheric pressure was injected through the calibration port of the gas chromatograph and the area was measured. The area was the calibration peak.

4.2.2 X-ray diffraction (XRD)

XRD were performed to determine the bulk phase of catalysts by SIEMENS D 5000 X-ray diffractometer connected with a computer with Diffract ZT version 3.3 program for fully control of the XRD analyzer. The experiments were carried out by using CuKα (λ = 1.54439 Å) radiation with Ni filter in the 2θ range of 20-80 degrees resolution 0.04^{o}. The crystallite size was estimated from line broadening according to the Scherrer equation and α-Al_2O_3 was used as standard.

4.2.3 Temperature programmed reduction (TPR)

TPR was used to determine the reducibility of catalysts:

1. The catalyst sample 0.2 g used in the sample cell.
2. Prior to operation, the catalysts were heated up to 200 ^{o}C in flowing nitrogen and held at this temperature for 1 h.
3. After the catalyst sample was cooled down to room temperature, carrier gas (10 % H_2 in Ar) were ramping from 35^{o}C to 800^{o}C.
4. During reduction, a cold trap will be placed to before the detector to remove water produced.

4.2.4 Electron microscopy

Scanning electron microscopy (SEM) and Energy dispersive X-ray spectroscopy (EDX) was used to determine the morphology and elemental distribution of the catalyst particles. Model of SEM: JEOL mode JSM-5800LV and EDX will be performed using Link Isis Series 300 program at the Scienctific and Technological Research Equipment Center, Chulalongkorn University (STREC).

4.2.5 Transmission Electron Microscopy (TEM)

The dispersion of cobalt oxide supports was determined using JEM-2100 transmission electron spectroscopy operated at 100 kV with 25 k magnification. The sample was dispersed in ethanol prior to the TEM measurement.

4.2.6 Hydrogen Chemisorption

Static H_2 chemisorption at 100 ^{o}C on the reduce catalysts was used to determine the number of reduce surface cobalt metal atoms and overall cobalt dispersion. The total hydrogen chemisorption was calculated from the number of injection of a known volume. H_2 chemisorption was carried out following the

procedure discribed by CO- pulse chemisorption technique using a Micrometritics Chemisorb 2750 (pulse chemisorption system). Prior to chemisorption, the catalysts were reduced at 350 ^{o}C for 3 hours after ramping up at a rate of 1 ^{o}C/min.

4.3. Reaction study in CO hydrogenation

4.3.1 Material

The reactant gas used for the reaction study was the carbon monoxide in hydrogen feed stream as supplied by Thai Industrial Gas Limited (TIG). The gas mixture contained 9.73 vol % CO in H_2 (22 cc/min). The total flow rate was 30 ml/min with the H_2/CO ratio of 10/1. Ultra high purity hydrogen (50 cc/min) and high purity argon (8 cc/min) manufactured by Thai Industrial Gas Limited (TIG) were used for reduction and balance flow rate.

4.3.2 Apparatus

Flow diagram of CO hydrogenation system is show in Figure 4.1. The system consists of a reactor, an automatic temperature controller, an electrical furnace and a gas controlling system.

4.3.2.1 Reactor

The reactor was made from a stainless steel tube (O.D. 3/8 “). Two sampling points were provided about and below the catalyst bed. Catalyst was placed between two quartz wool layers.

4.3.2.2 Automation Temperature Controller

This unit consisted of a magnetic switch connected to a variable voltage transformer and a solid state relay temperature controller model no.SS2425DZ connected to a thermocouple. Reactor temperature was measured at the bottom of the catalyst bed in the reactor. The temperature control set point is adjustable within the rang of 0-800 ^{o}C at the maximum voltage output of 220 volt.

4.3.2.3 Electrical Furnace

The furnace supplied heat to the reactor for CO hydrogenation. The reactor could be operated from temperature up to 800 ^{o}C at the maximum voltage of 220 volt.

4.3.2.4 Gas Controlling System

Reactant for the system was each equipped with a pressure regulator and an on-off valve and the gas flow rates were adjusted by using metering valves.

4.3.2.5 Gas Chromatograph

The composition of hydrocarbons in the product stream was analyzed by a Shimadzu GC-14B (VZ10) gas chromatograph equipped with a flame ionization detector. A Shimadzu GC-8A (molecular sieve 5A) gas chromatograph equipped with a thermal conductivity detector was used to analyze CO and H_2 in the feed and product streams. The operating conditions for each instrument are show in the Table 4.2.

4.3.3 Procedured

1. Using 0.2 g of catalyst packed in the middle of the stainless steel micro reactor, which is located in the electrical furnace.

2. A flow rate of Ar = 8 cc/min, 9% CO in H_2 = 22 cc/min and H_2 = 50 cc/min in a fixed-bed flow reactor. A relatively high H_2/CO ratio was used to minimize deactivation due to carbon deposition during reaction.

3. The catalyst sample will be re-reduced *in situ* in flowing H_2 at 350^{o}C for 10 h prior to CO hydrogenation.

4. CO hydrogenation will be carried out at 220^{o}C and 1 atm total pressure in flowing 9% CO in H_2.

5. The effluent was analyzed using gas chromatography technique [Thermal conductivity detector (TCD) will be used for separation of carbon monoxide (CO) and methane (CH_4) and flame ionization detector (FID) will be used for

separation of light hydrocarbon such as methane (CH_4), ethane (C_2H_6), propane (C_3H_8), etc.] In all cases, steady-state was reached within 5 h.

Table 4.2 Operating condition for gas chromatograph

Gas Chromatograph	SHIMADZU GC-8A	SHIMADZU GC-14B
Detector	TCD	FID
Column	Molecular sieve 5A	VZ 10
- Column material	SUS	-
- Length	2 m	-
- Outer diameter	4 mm	-
- Inner diameter	3 mm	-
- Mesh range	60/80	60/80
- Maximum temperature	350 ^oC	80^oC
Carrier gas	He (99.999%)	N_2 (99.999%)
Carrier gas flow	20 cc/min	-
Column gas	He (99.999%)	Air , H_2
Column gas flow	20 cc/min	-
Column temperature		
- initial (^oC)	60	70
- final (^oC)	60	70
Injector temperature (^oC)	100	100
Detector temperature (^oC)	100	150
Current (mA)	80	-
Analysed gas	Ar, CO, H_2	Hydrocarbon C_1-C_4

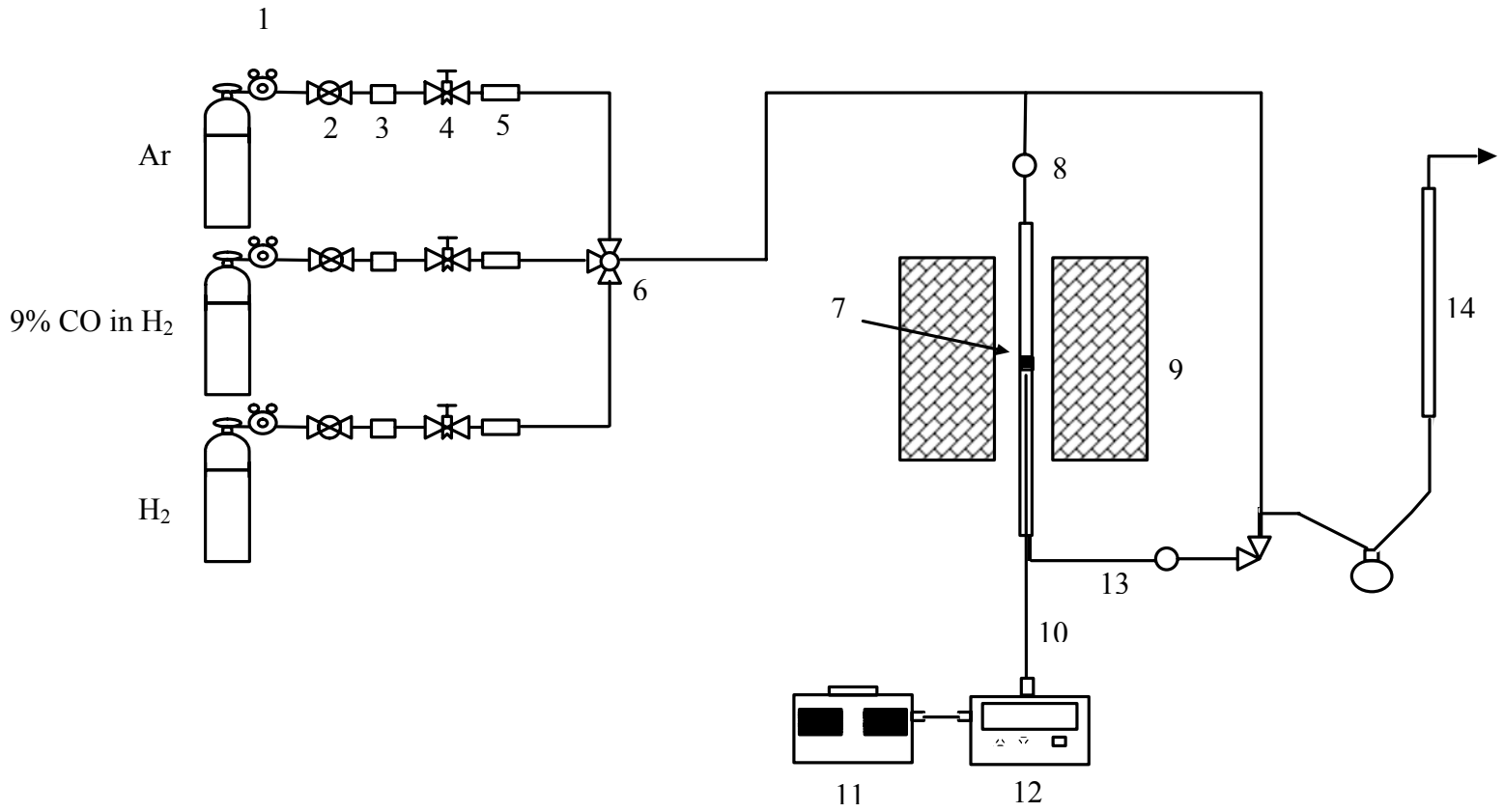

1. Pressure Regulator
2. On-Off Value
3. Gas Filter
4. Metering Valve
5. Back Pressure
6. 3-way Valve
7.Catalyst Bed
8. Sampling point
9. Furnace
10. Thermocouple
11. Variable Voltage Transformer
12. Temperature Controller
13. Heating Line
14. Bubble Flow Meter

Figure 4.1 Flow diagram of CO hydrogenation system

RESEARCH METHODOLOGY

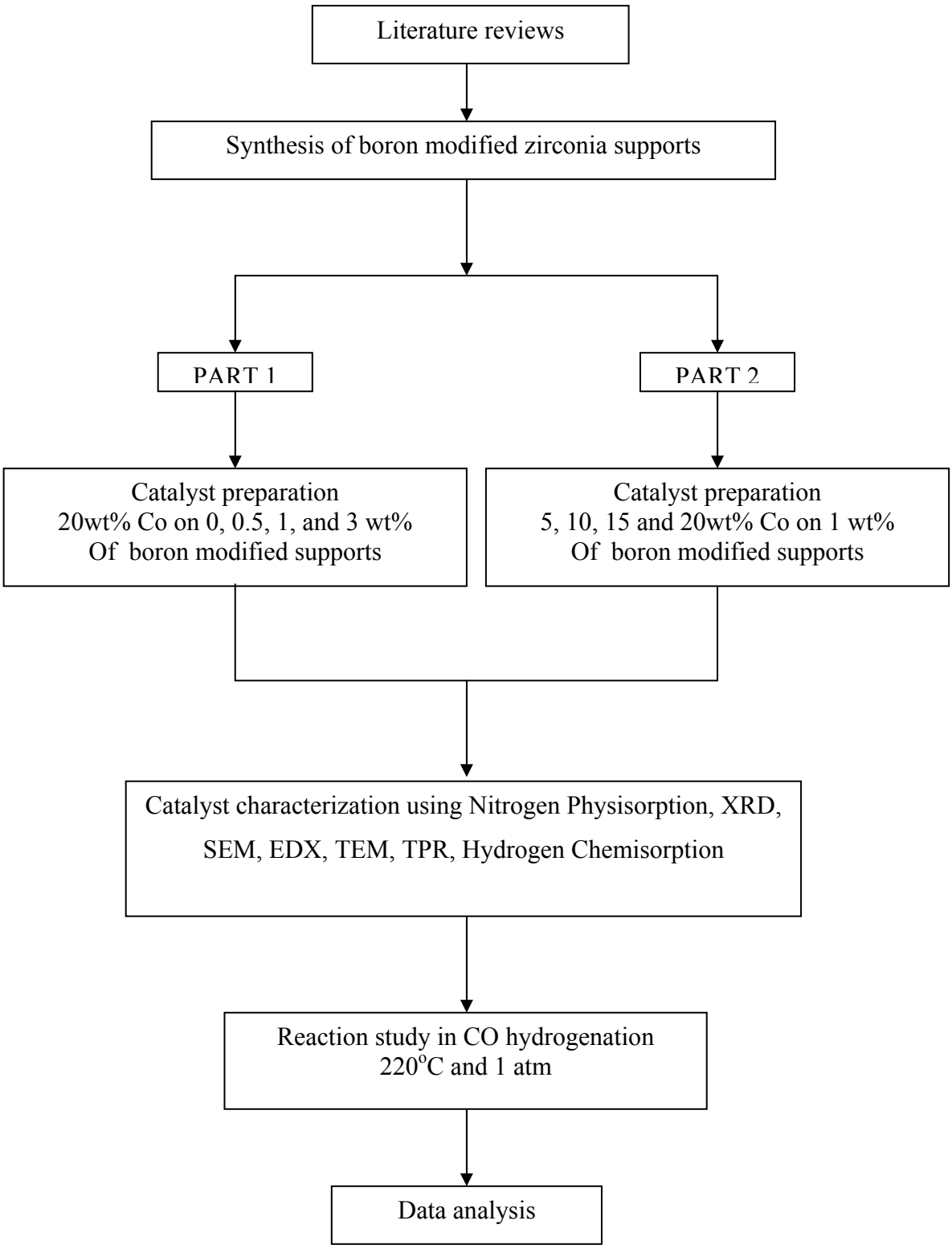

CHAPTER V

RESULTS AND DISCUSSION

In this chapter are divided into two sections. Section 5.1 is described characteristics of 20 wt% cobalt (Co) dispersed on various boron modified supports. Section 5.2 described characteristics and catalytic activity toward CO hydrogenation of various Co catalysts dispersed on 1 wt% of boron modified support.

5.1 Various boron loading of 20 wt% cobalt on boron modified zirconia-supported catalysts.

5.1.1 BET surface area

The BET surface area are listed in **Table 5.1**. The BET surface areas of B-modified zirconia supports decreased from 2.6 to 1.1 m^2/g upon increasing the amounts of boron loading**.** The pore size distributions of the unmodified and B-modified zirconia support are shown in **Figure 5.1**. In fact, the slightly bimodal pore size distribution for the unmodified zirconia support was observed. However, with the B modification, the unimodal pore size distribution of the B-modified zirconia supports was evident. It indicated that B was presumably located in the small pore of zirconia support resulting in the disappearance of the small pore portion as seen in **Figure 5.1**. Considering the surface areas of the zirconia-supported cobalt catalysts with B modification, they apparently increased from 1.8 to 12.6 m^2/g with increasing the amounts of B loading in the zirconia supports. This was suggested that the B modification could prevent the agglomeration of Co oxide species resulting in increased surface areas of the catalyst samples.

Table 5.1 BET surface area measurement of 20 wt% cobalt on boron modified supported cobalt catalyst.

Samples	BET Surface Area (m^2/g) [a]
ZrB-0	2.6
ZrB-0.5	1.8
ZrB-1	1.3
ZrB-3	1.1
20-Co/ZrB-0	1.8
20-Co/ZrB-0.5	6.8
20-Co/ZrB-1	12.4
20-Co/ZrB-3	12.6

[a] Measurement error is ±5%

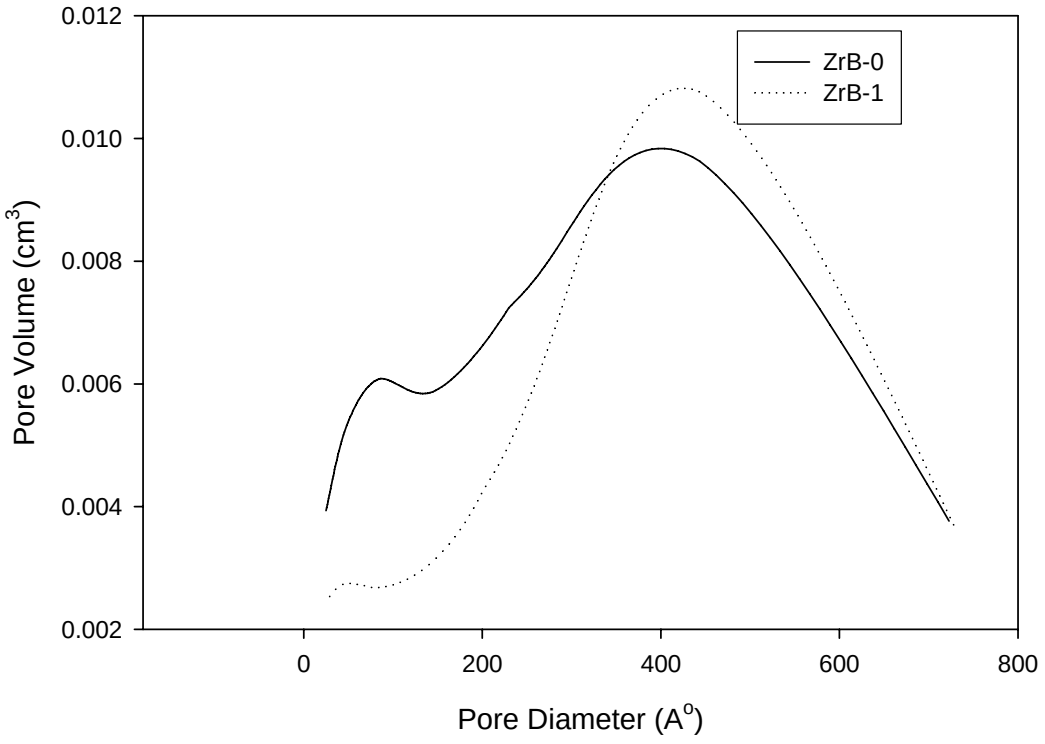

Figure 5.1 Pore size distribution of supports

5.1.2 X-ray diffraction (XRD)

The XRD patterns for different zirconia supports consisting of various amounts of boron loading are shown in **Figure 5.2**. The unmodified zirconia support exhibited the strong XRD peaks at 29° and 32° assigning to the ZrO_2 in the monoclinic phase, and the strong XRD peak at 50° indicating the ZrO_2 in the tetragonal phase. In addition, the strong XRD peak at 29° (overlap with the XRD peak for the monoclinic phase of ZrO_2) was detected for the zirconia supports with B modification also assigning to the B_2O_3 species. **Figure 5.3** shows the XRD patterns of different zirconia-supported cobalt catalysts consisting of various amounts of B loading in the zirconia supports. The catalyst samples exhibited XRD peaks at 36°, 45°, 60° and 65° indicating the presence of Co_3O_4 species.

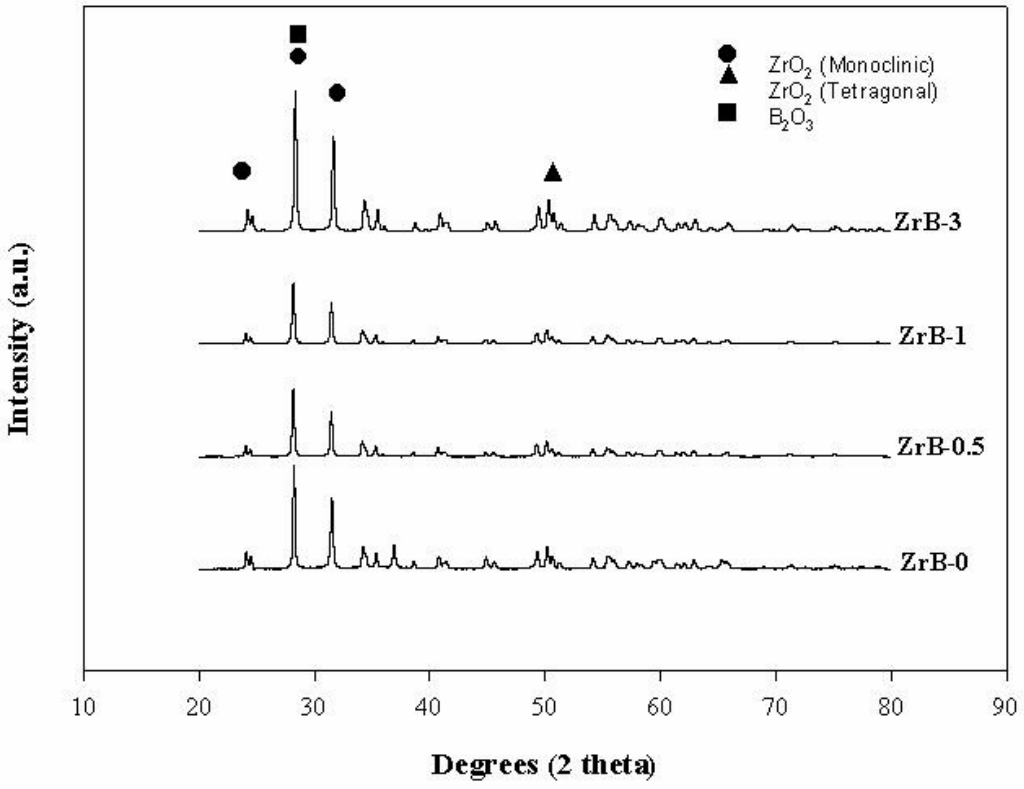

Figure 5.2 XRD patterns for different ZrO_2 supports consisting of various amounts of boron loading

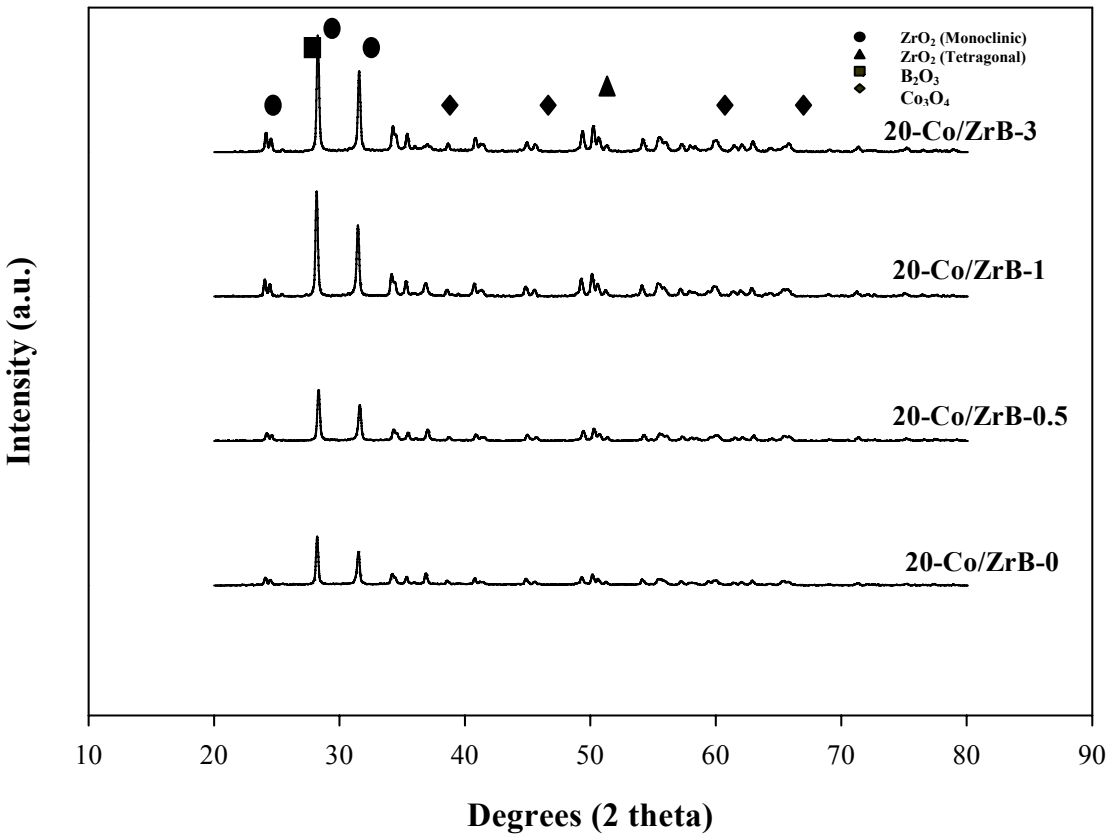

Figure 5.3 XRD patterns for different Co/ZrO_2 catalysts with various amounts of boron modification on zirconia support

5.1.3 Scanning electron microscopy (SEM) and Energy dispersive X-ray spectroscopy (EDX)

In order to study the morphologies and elemental distribution of the catalyst samples, SEM and EDX were performed, respectively. The SEM micrograph and the elemental distribution for Co, Zr, and O for the unmodified zirconia-supported Co catalyst are shown in **Figure 5.4** whereas the typical SEM micrograph and the elemental distribution for the B-modified zirconia-supported Co catalysts are shown in **Figure 5.5-5.7**. For all figures, it was found that the distribution of Co oxide species was well distributed all over the catalyst granule.

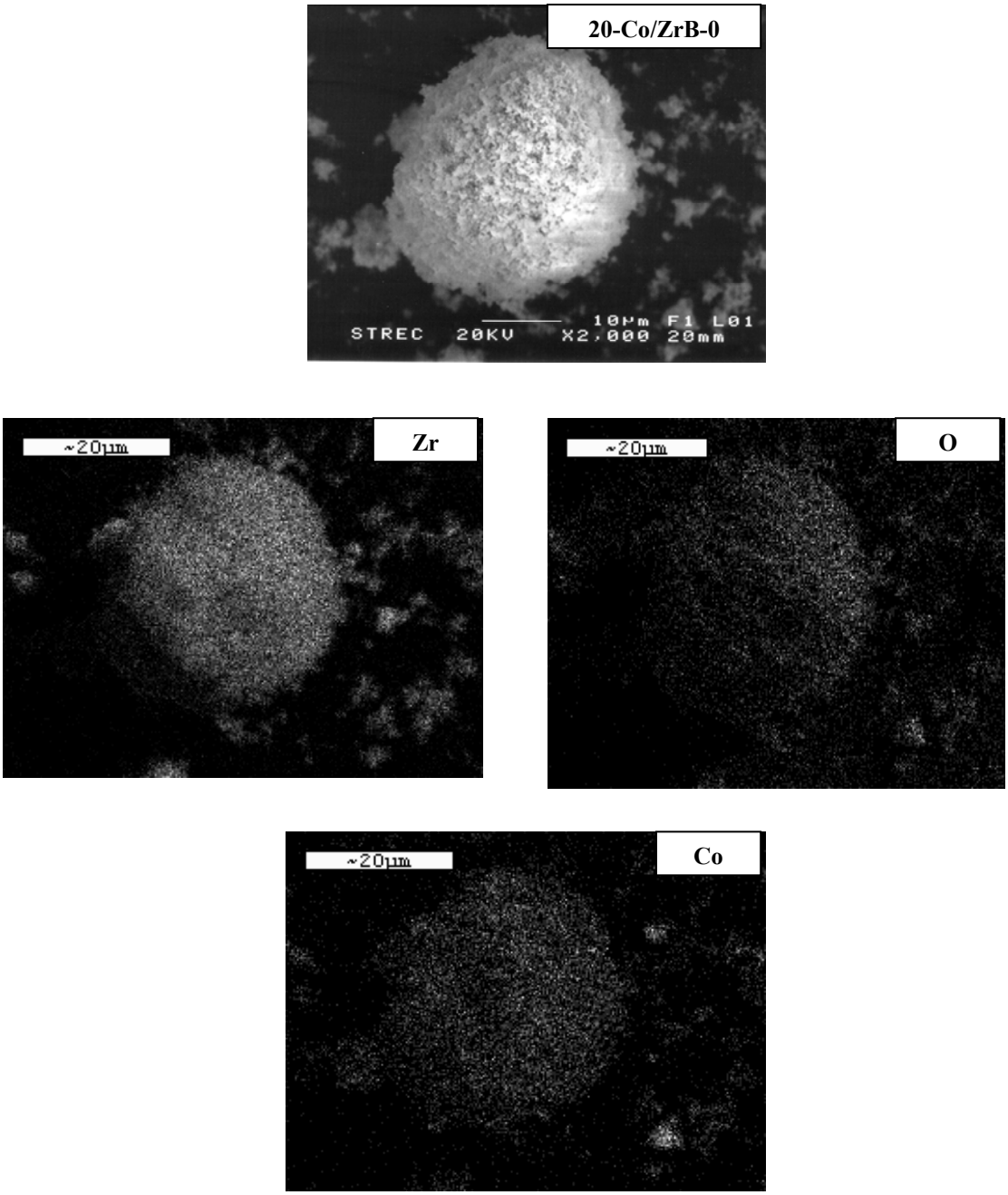

Figure 5.4 A typical SEM micrograph and EDX mapping for 20-Co/ZrB-0 sample

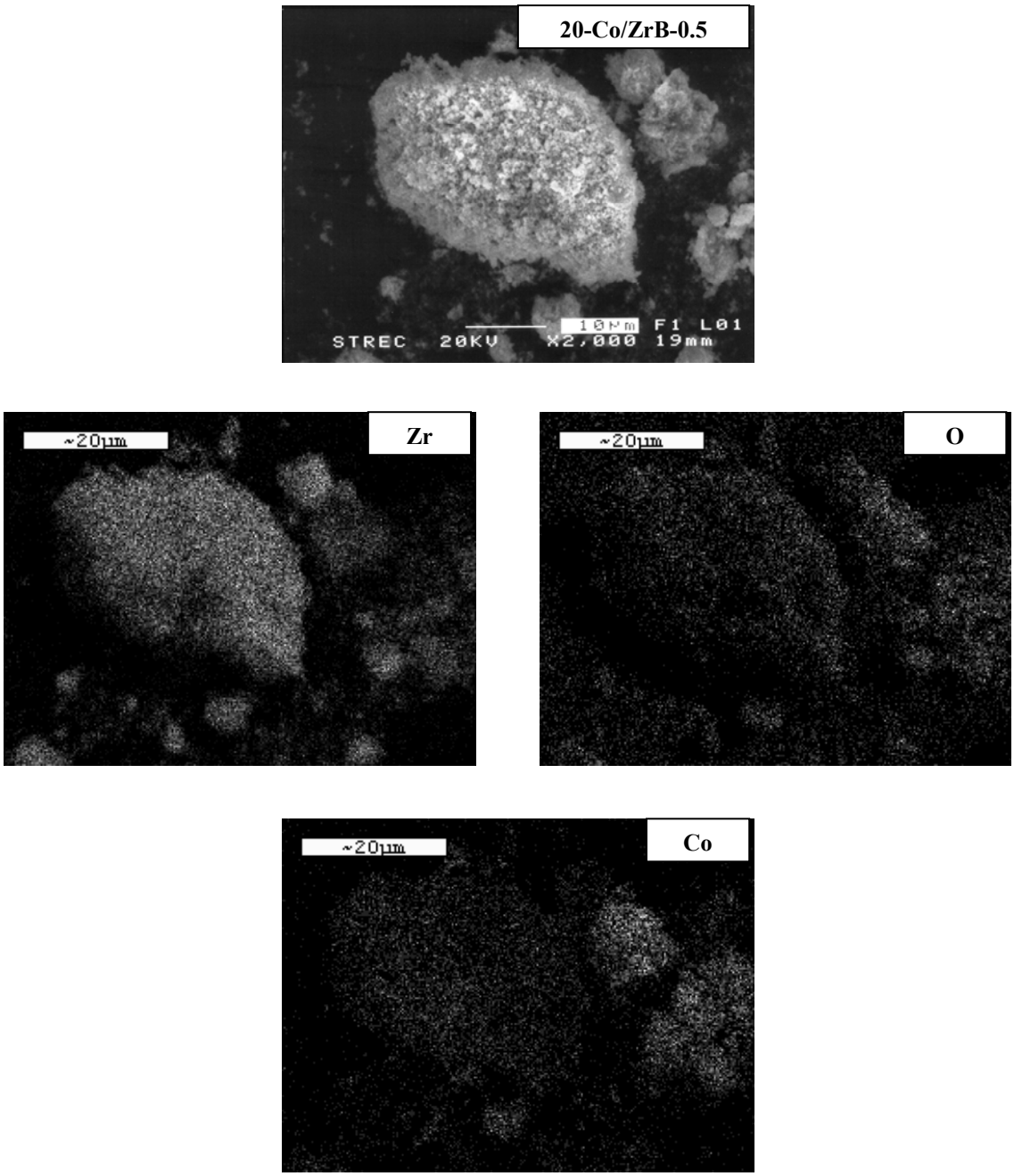

Figure 5.5 A typical SEM micrograph and EDX mapping for 20-Co/ZrB-0.5 Sample

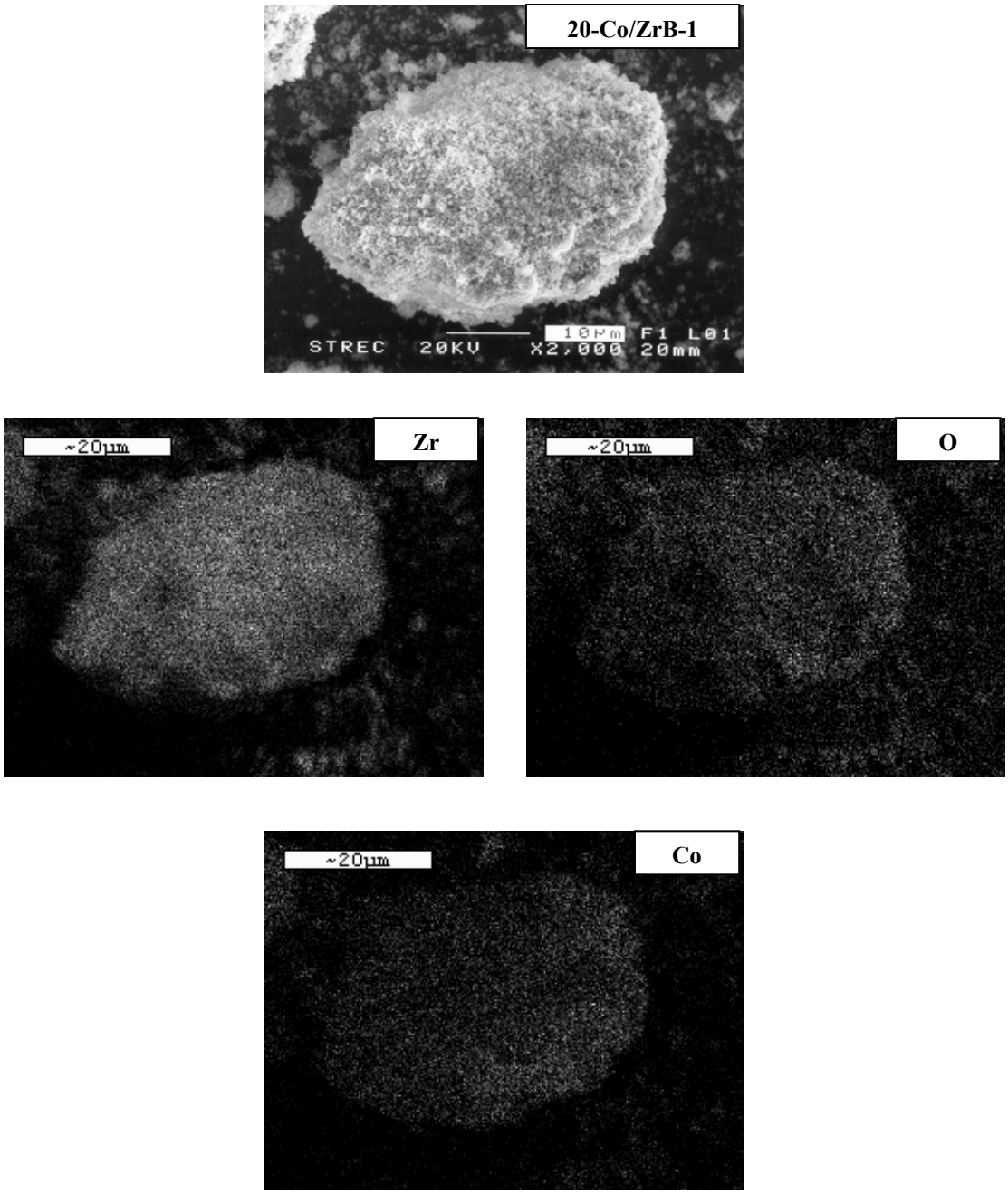

Figure 5.6 A typical SEM micrograph and EDX mapping for 20-Co/ZrB-1 sample

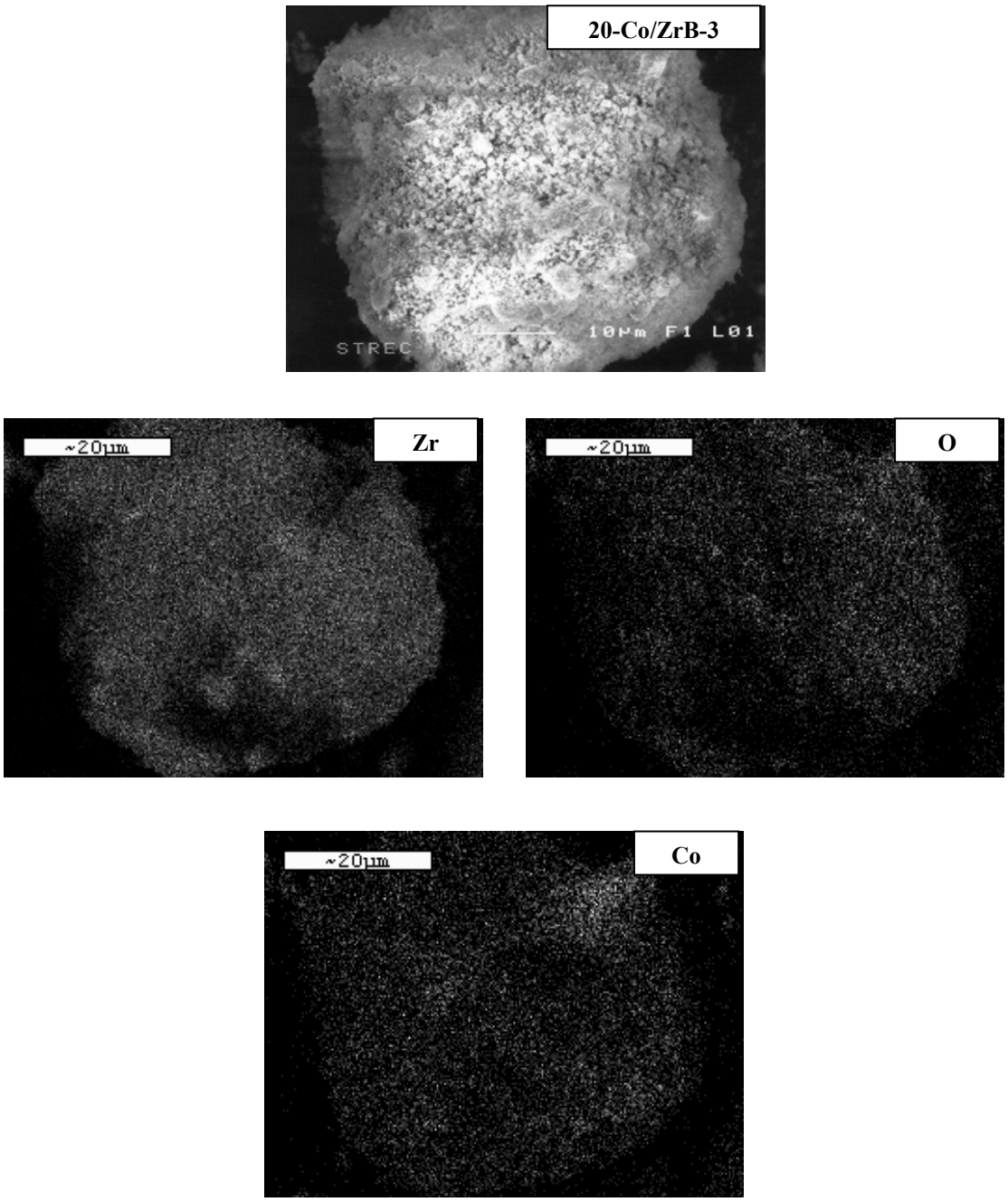

Figure 5.7 A typical SEM micrograph and EDX mapping for 20-Co/ZrB-3 sample

5.1.4 Transmission Electron Microscopy (TEM)

In order to determine the dispersion and crystallite size of Co oxides species dispersed on the various supports employed, the high resolution TEM was used. The TEM micrographs for the unmodified and B-modified zirconia supports are shown in **Figure 5.8**. There was no significant change in morphologies of the zirconia supports upon B modification. The dispersion of Co oxide species on various zirconia supports is illustrated in **Figure 5.9**. It can be observed that the dispersion of Co oxide species apparently increased with increasing the amounts of B loading in the zirconia support resulting in the smaller size of the Co oxides present.

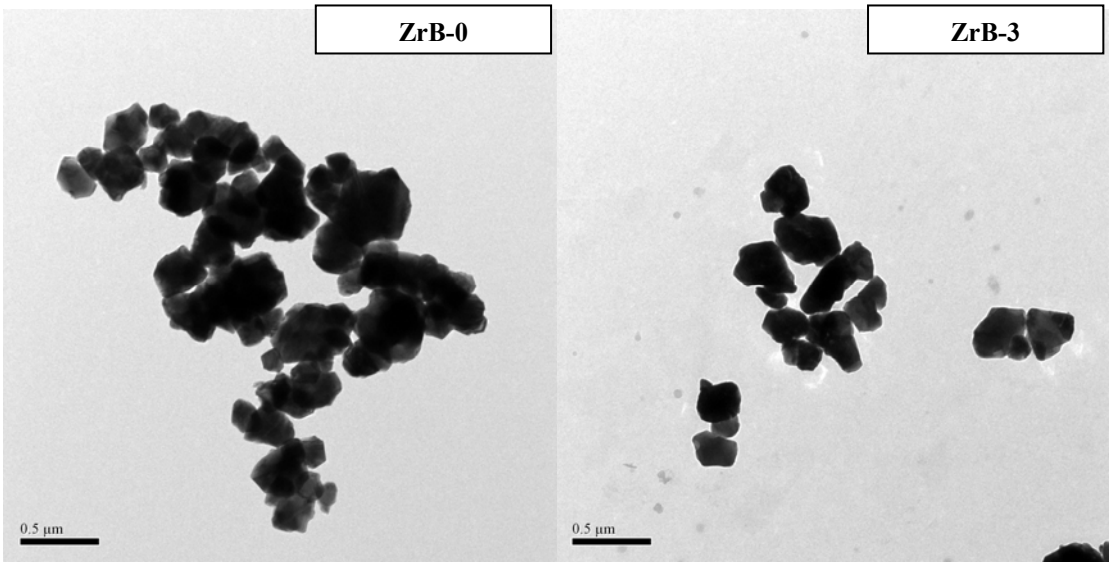

Figure 5.8 TEM micrographs for different ZrO_2 supports consisting of various amounts of boron loading

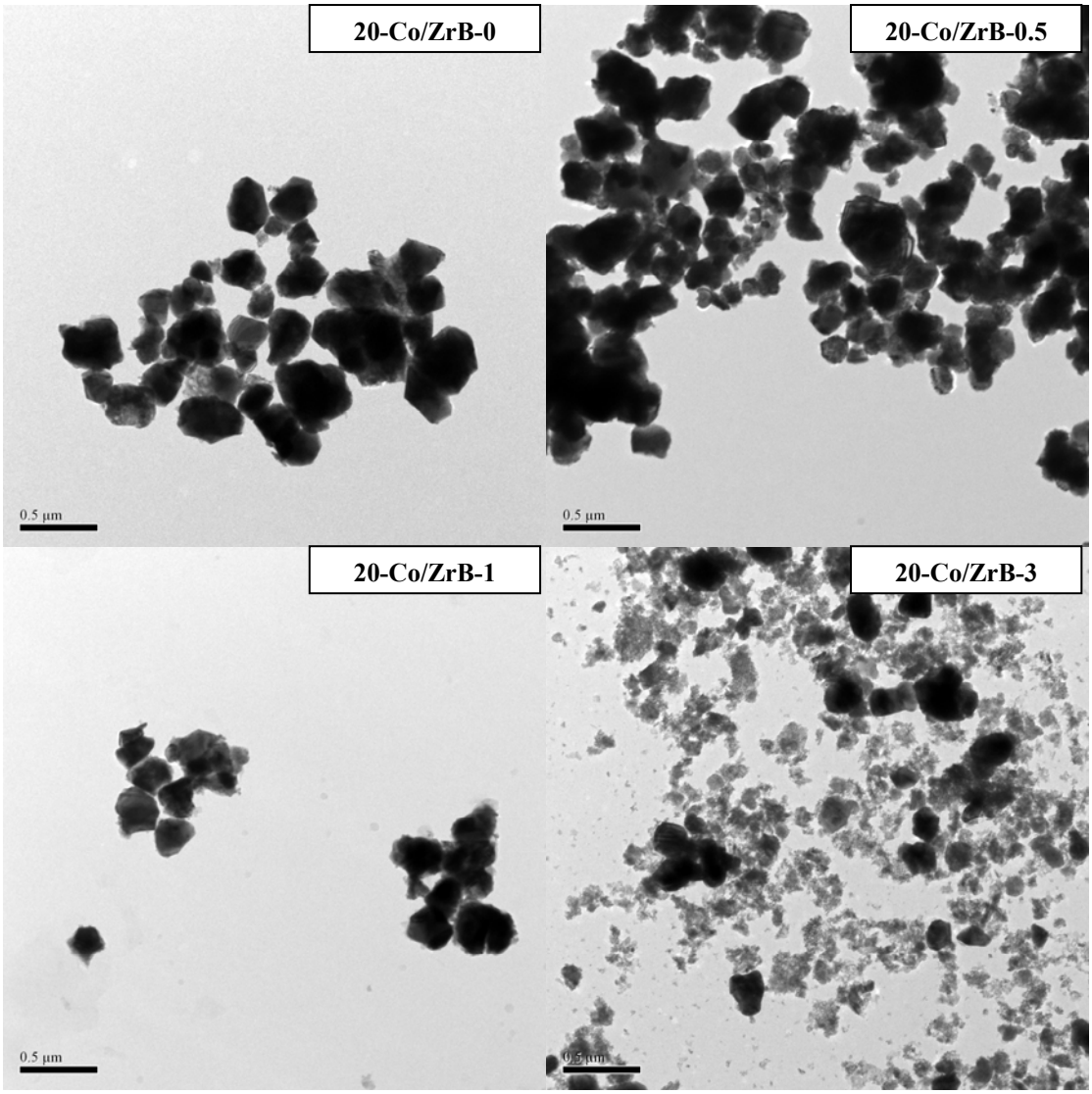

Figure 5.9 TEM micrographs for different Co/ZrO_2 catalysts with various amounts of boron modification on zirconia support

5.1.5 Temperature programmed reduction (TPR)

The TPR measurement was performed in order to determine the reduction behaviors of Co oxides species on various samples. The TPR profiles of various zirconia-supported Co catalysts with and without B modification on zirconia supports are shown in **Figure 5.10** and the reduction temperatures are listed in **Table 5.2**. Basically, only two reduction peaks can be observed. The peaks can be assigned to the two-step reduction of Co_3O_4 to CoO and then to Co^0 (Y. Zhang et al., 1999; D. Schanke et al., 1995). Upon the TPR conditions, the two reduction peaks based on

two-step reduction may or may not be observed. Here, for the unmodified zirconia-supported Co catalyst, the broad reduction peak (ca.230-490^{o}C) having a little shoulder (ca. 300^{o}C) can be observed assigning to the overlap of two-step reduction. However, with the B modification we found that the reduction peaks were shifted to the higher reduction temperatures. It was suggested that the B-modification can result in lower degree of reduction, especially with high amounts (3 wt%) of B loading on the zirconia supports. The smaller size of Co oxide species, the more difficult of them to be reduced. So, boron could increase the interaction between Co_3O_4 and ZrO_2. In addition, the effect of boron may result in the formation of a surface cobalt-boron compound which is more difficult to reduce (J. Li *et al*., 1999). Thus the reducibility of Co/ZrO_2 directly reflects the interaction between Co_3O_4 and the B sources. However, it should be noted that TPR conditions were different from the standard reduction used prior to reaction.

Table 5.2 Reduction temperature of catalyst samples

Catalyst Samples	Reduction Temperature (^{o}C)		
	Initial	**Final**	**Maximum**
20-Co/ZrB-0	230	490	420
20-Co/ZrB-0.5	330	760	450
20-Co/ZrB-1	350	770	570
20-Co/ZrB-3	560	800	750

5.1.6 H_2 chemisorption

H_2 chemisorption was performed in order to measure the number of reduced cobalt metal surface atoms, which is related to the overall activity during CO hydrogenation. The resulted H_2 chemisorption is illustrated in **Table 5.3**. The amounts of H_2 adsorbed on the catalytic phase were in the range of 0.33 to 0.47 μmol/g of sample. It was found that the number of the reduced cobalt metal surface atoms was the largest for the cobalt dispersed on the 20 wt% of Co on 1 wt% of boron modified zirconia support (20-Co/ZrB-1).

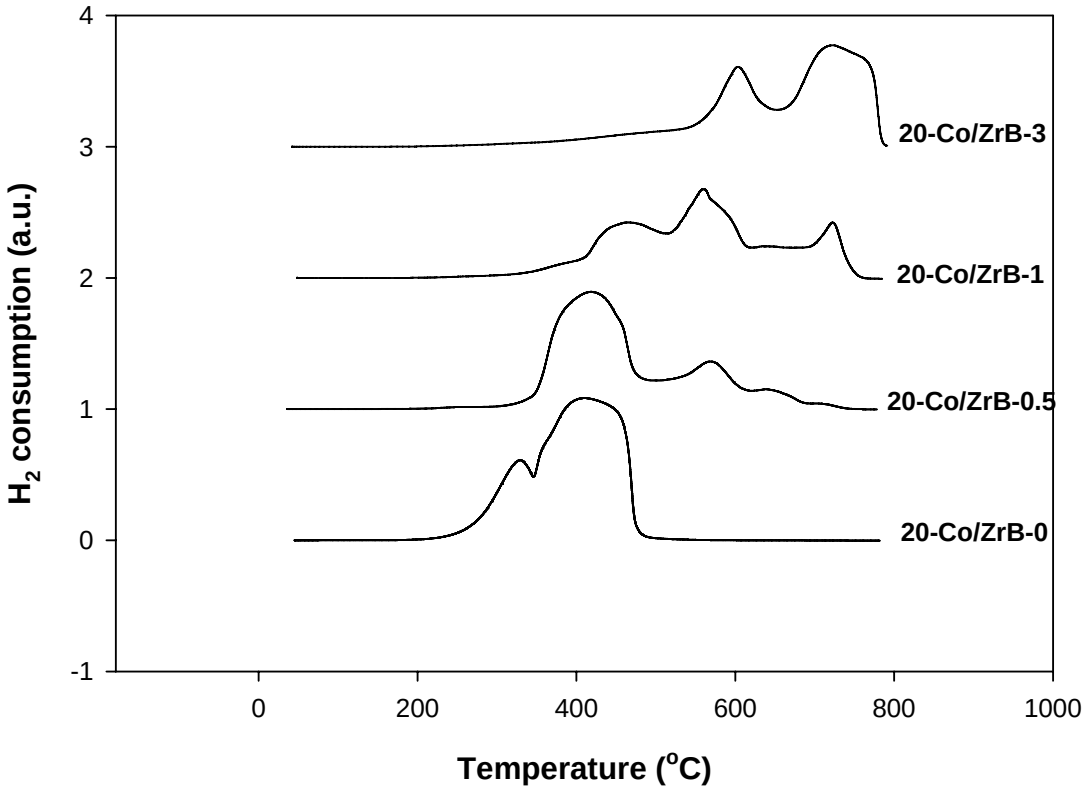

Figure 5.10 TPR profiles for different Co/ZrO_2 catalysts with various amounts of boron modification on zirconia support

5.1.7 Reaction study in CO hydrogenation

The reaction study under CO hydrogenation was also investigated in order to measure the activity and selectivity of catalysts. The reaction study results are listed in **Table 5.3.** It was obvious that the catalytic activities of the zirconia-supported Co catalyst dramatically increased about 6-8 times with B modification on the zirconia supports. Increased activities upon B modification can be attributed to increased dispersion of Co oxide species as seen from TEM measurement. This was suggested that the higher degree dispersion of Co oxide species could facilitate the reduction of Co oxides giving the higher number of the Co metal surface atoms for catalyzing the reaction. However, it should be carefully noted that too small crystallite sizes of Co oxides, which were corresponding to the amounts of B loading of 0.5 and 3 wt%, respectively essentially decreased the degree of reduction resulting in a slight decrease in activity. The similar phenomenon was also discussed for the

dispersion of Co oxide species on titania supports consisting of various ratios of anatase and rutile phases (B. Jongsomjit *et al*., 2005). It was reported that highly dispersed forms of Co oxide species were not only the factor to insure larger number of reduced Co metal surface atoms. Considering the product selectivity upon methanation condition as seen in **Table 5.3**, it was found that the selectivity to C_2-C_4 products slightly decreased with the B modification on the zirconia supports.

Table 5.3 Results of H_2 chemisorption, steady-state rate and selectivity to products

Catalyst Sample	**Total H_2 chemisorption (µmol/g cat)**	**Steady-state Rate[a] (x10^{2}gCH_2/gcat.h)**	**CH_4 Selectivity (%)**	**C_2-C_4 Selectivity (%)**
20-Co/ZrB-0	0.33	3.0	96.5	3.5
20-Co/ZrB-0.5	0.44	20.2	99.0	1.0
20-Co/ZrB-1	0.47	25.2	99.0	1.0
20-Co/ZrB-3	0.34	22.7	98.9	1.1

[a] CO hydrogenation was carried out at 220^{o}C, 1 atm and H_2/CO/Ar = 20/2/8. The steady-state was reached after 5 h.

It has been reported that addition of a small amount of second metal such as silicon and yttrium can improve the properties of nanocrystalline zirconia supported cobalt catalyst. For example, when used as cobalt catalyst supports the Si- and Y- modified zirconia supported ones with Si/Zr > 0.005 and Y/Zr > 0.01 exhibited higher H_2 chemisorption and CO hydrogenation activities. It was found that the CO hydrogenation rates increased by 1.2-1.6 times with the Si- and Y- modified zirconia(P. Soisuwan *et al.*, 2006). However, we found that the CO hydrogenation rates increased by 6-7 times with the B- modified microcrystalline zirconia supported cobalt catalyst.

5.2 Various Co loading on the 1 wt% boron modified zirconia supported catalyst.

5.2.1 BET surface area

The BET surface area are listed in **Table 5.4**. The BET surface areas of the zirconia-supported cobalt catalysts with 1 wt% of B modification increased from 4.0 to 12.4 m^2/g upon increasing the amounts of cobalt loading**.** This was suggested the Co oxide species exhibited well distribution, leading to increased surface areas of the catalyst samples.

Table 5.4 BET surface area measurement of various cobalt on 1wt% of boron modified supported cobalt catalyst.

Samples	BET Surface Area (m^2/g) [a]
5-Co/ZrB-1	4.0
10-Co/ZrB-1	10.0
15-Co/ZrB-1	12.2
20-Co/ZrB-1	12.4

[a] Measurement error is ±5%

5.2.2 X-ray diffraction (XRD)

The XRD patterns for different zirconia supported cobalt catalysts consisting of various amounts of cobalt loading are shown in **Figure 5.11**. The catalyst samples exhibited the strong XRD peaks at 29^o and 32^o assigning to the ZrO_2 in the monoclinic phase, the strong XRD peak at 50^o indicating the ZrO_2 in the tetragonal phase and the strong XRD peak at 29^o (overlap with the XRD peak for the monoclinic phase of ZrO_2) was detected for the zirconia supports with B modification also assigning to the B_2O_3 species. In addition**,** the XRD peaks at 36^o, 45^o, 60^o and 65^o indicating the presence of Co_3O_4 species.

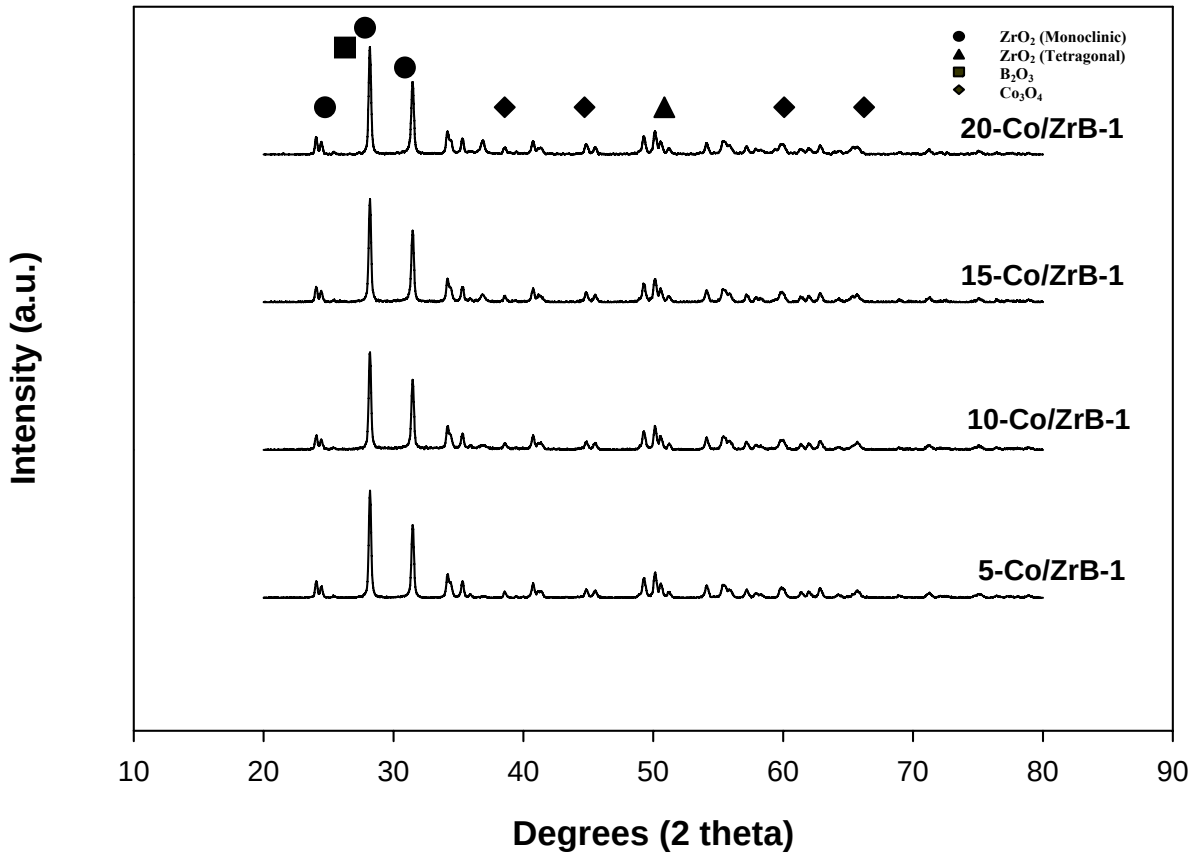

Figure 5.11 XRD patterns of the 1 wt% of boron-modified zirconia supported Co catalyst.

5.2.3 Scanning electron microscopy (SEM) and Energy dispersive X-ray spectroscopy (EDX)

SEM and EDX were also conducted in order to study the morphologies and elemental distribution of the samples, respectively. The SEM micrograph and the elemental distribution for Co, Zr, and O for the 1 wt% of boron modified supported Co catalysts are illustrated in **Figure 5.12-5.15.** For all figures, it was found that the distribution of Co oxide species was well distributed all over the catalyst granule**.**

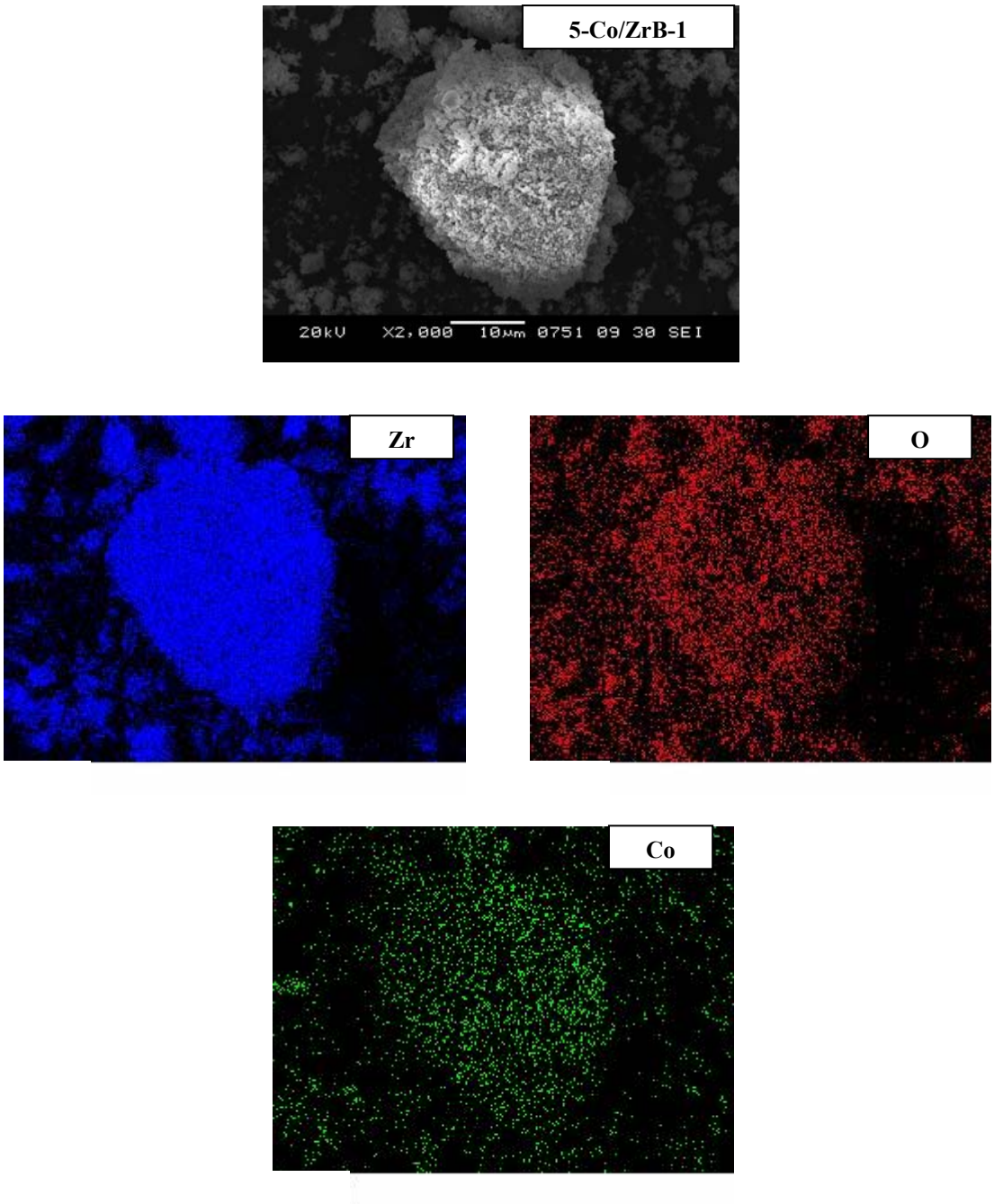

Figure 5.12 A typical SEM micrograph and EDX mapping for 5-Co/ZrB-1 sample

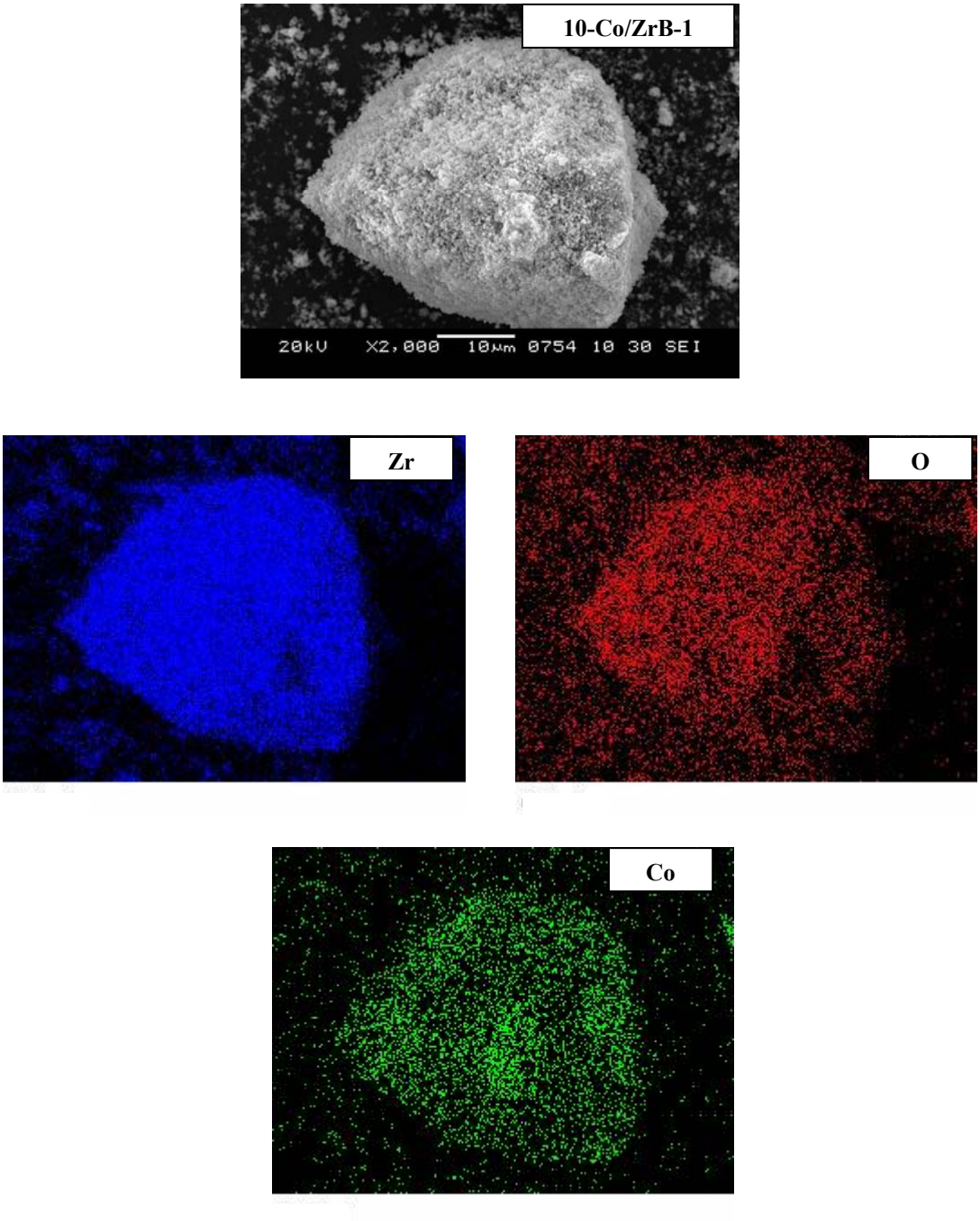

Figure 5.13 A typical SEM micrograph and EDX mapping for 10-Co/ZrB-1 sample

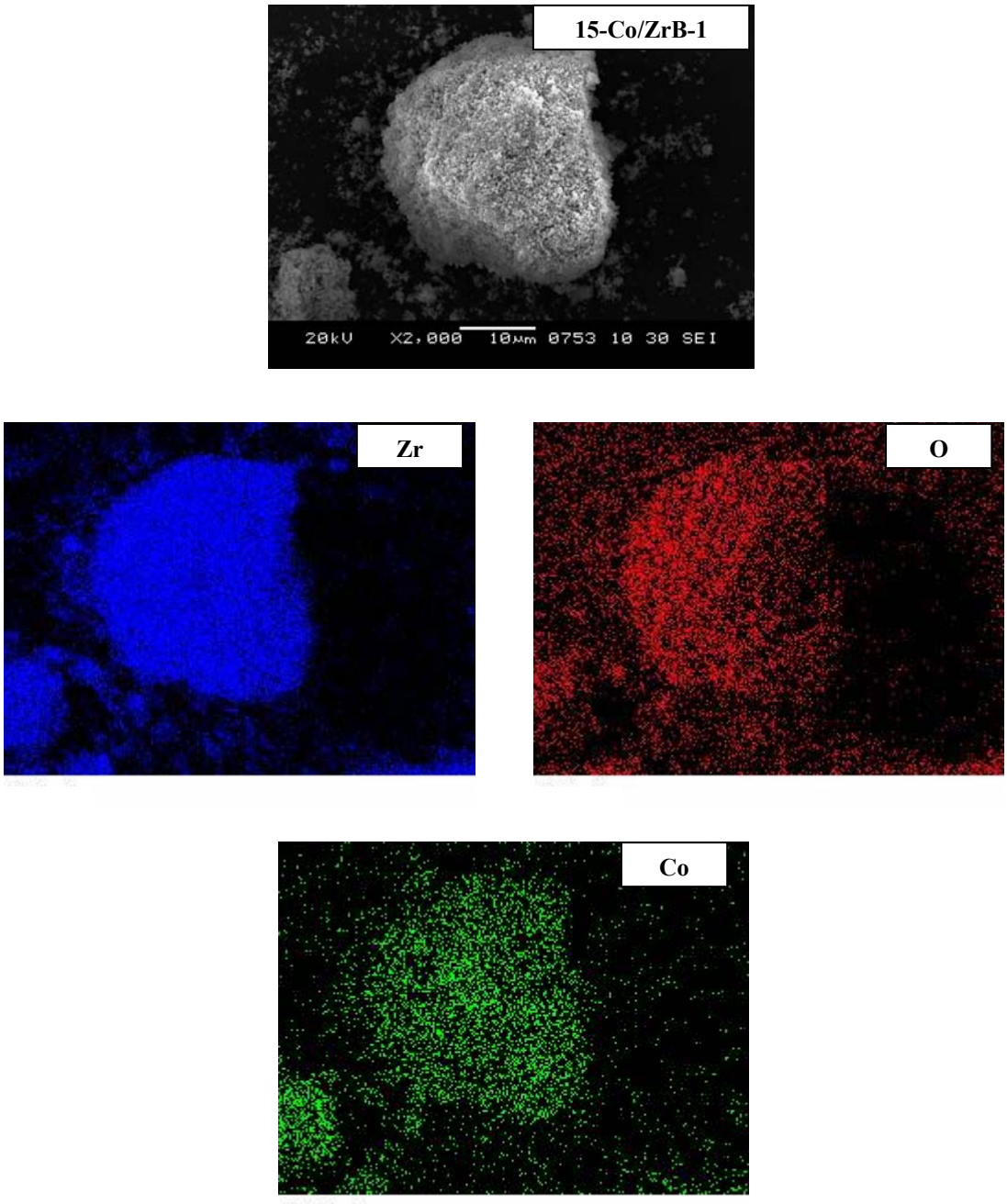

Figure 5.14 A typical SEM micrograph and EDX mapping for 15-Co/ZrB-1 Sample

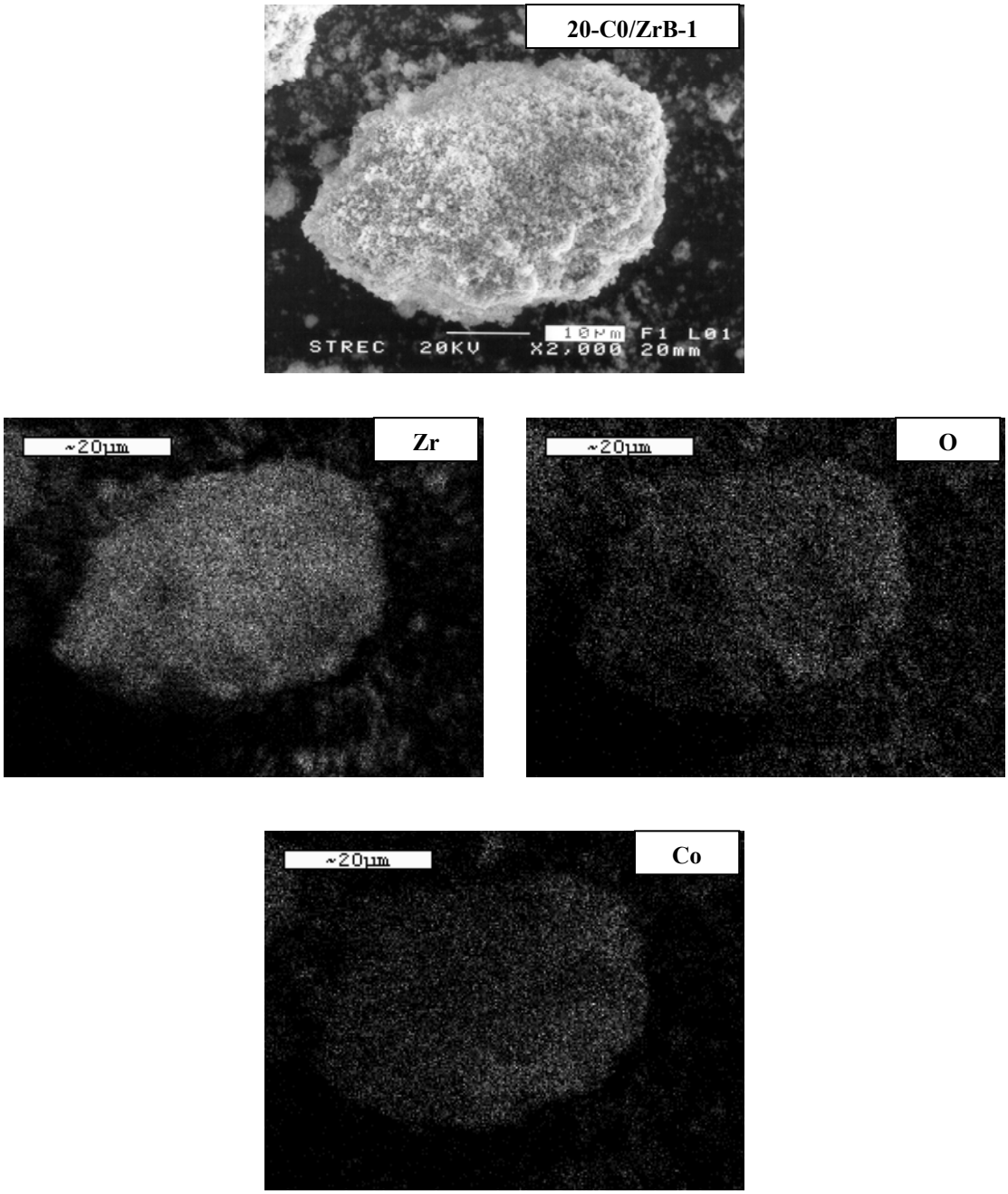

Figure 5.15 A typical SEM micrograph and EDX mapping for 20-Co/ZrB-1 sample

5.2.4 Transmission Electron Microscopy (TEM)

In order to determine the dispersion and crystallite size of Co oxides species dispersed on the various amounts of Co loading in the 1 wt% of boron modified supported catalysts employed, the high resolution TEM was used. The TEM micrographs for the catalysts are shown in **Figure 5.16**. It can be observed that the dispersion of Co oxide species apparently increased with increasing the amounts of Co loading in the 1 wt% of boron-modified zirconia supported Co catalysts resulting in the smaller size of the Co oxides present.

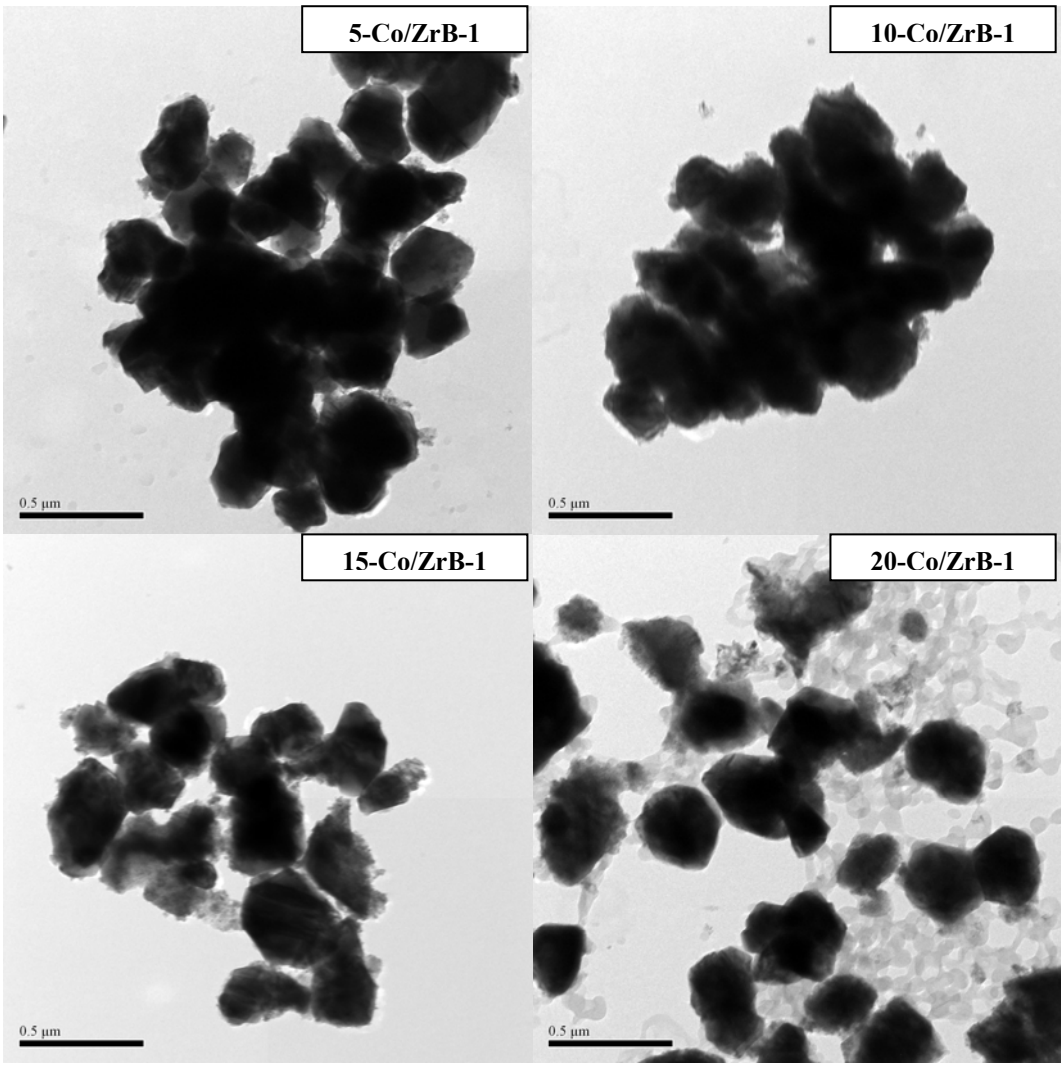

Figure 5.16 TEM micrographs for different Co/ZrO_2 catalysts with various amounts of Co loading on 1 wt% of boron-modified zirconiasupported Co catalysts

5.2.5 Temperature programmed reduction (TPR)

The TPR measurement was performed in order to determine the reduction behaviors of Co oxides species on various samples. The TPR profiles of various zirconia-supported Co catalysts with 1 wt% of B modification on zirconia supports are shown in **Figure 5.17** and the reduction temperatures are listed in **Table 5.5**. Basically, only two reduction peaks can be observed. The peaks can be assigned to the two-step reduction of Co_3O_4 to CoO and then to Co^0 (Y. Zhang et al., 1999; D. Schanke et al., 1995). Upon the TPR conditions, the two reduction peaks based on two-step reduction may or may not be observed. Here, for the 1 wt% of B modification zirconia-supported Co catalyst decreased in cobalt loading on zirconia support resulted in deceasing cobalt oxide on supports, then being more difficult for such the Co oxide species to be reduced with the small amount cobalt loading. However, with the 1 wt% of B modification, increased Co loading apparently resulted in the shift to the lower reduction temperatures. It was suggested that the smaller size of Co oxide species, the less difficult of them to be reduced. However, it should be noted that TPR conditions were different from the standard reduction used prior to reaction.

Table 5.5 Reduction temperature of catalyst samples

Catalyst Samples	Reduction Temperature (^oC)		
	Initial	**Final**	**Maximum**
5-Co/ZrB-1	406	724	682
10-Co/ZrB-1	500	694	555
15-Co/ZrB-1	370	739	478
20-Co/ZrB-1	350	770	570

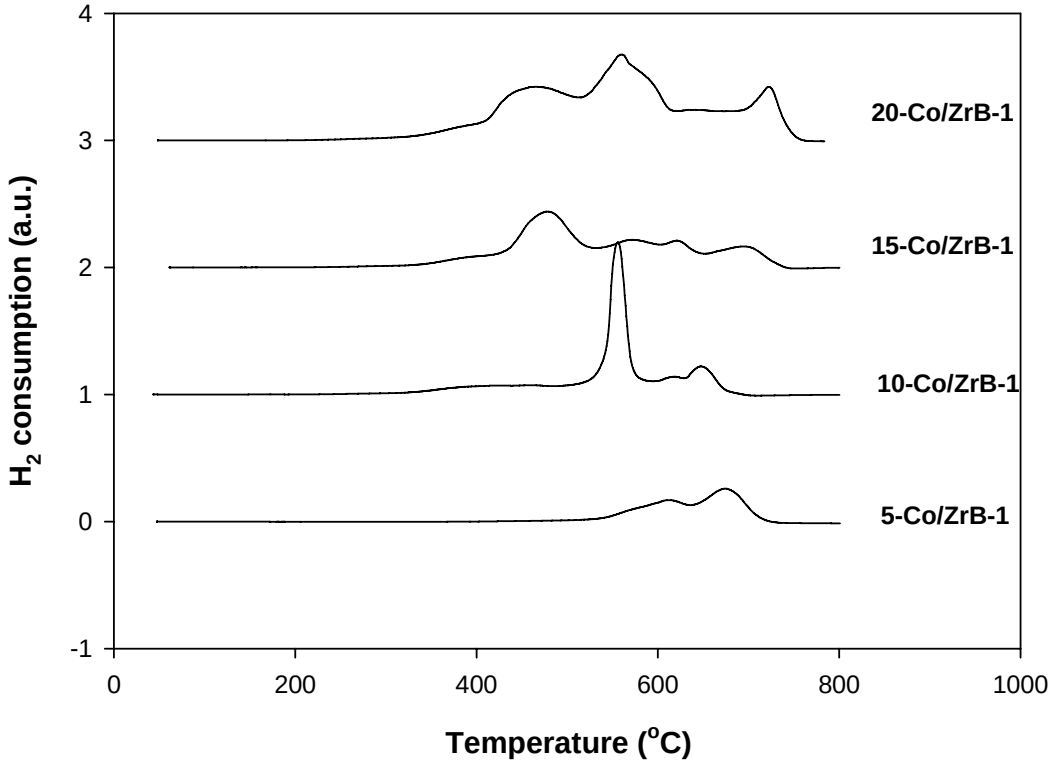

Figure 5.17 TPR profiles for the 1 wt% of boron modified-supported Co catalyst.

5.2.6 H_2 chemisorption

H_2 chemisorption was performed in order to measure the number of reduced cobalt metal surface atoms, which is related to the overall activity during CO hydrogenation. The resulted H_2 chemisorption is illustrated in **Table 5.6**. The amounts of H_2 adsorbed on the catalytic phase were in the range of 0.04 to 0.47 μmol/g of sample. It was found that the number of the reduced cobalt metal surface atoms was the largest for the cobalt dispersed on the 20 wt% of Co on 1 wt% of boron modified zirconia support (20-Co/ZrB-1).

5.2.7 Reaction study in CO hydrogenation

The reaction study under CO hydrogenation was also investigated in order to measure the activity and selectivity of catalysts. The reaction study results are listed in **Table 5.6.** Increased activities upon Cobalt loading can be attributed to increased dispersion of Co oxide species as seen from TEM measurement. This was

suggested that the higher degree dispersion of Co oxide species could facilitate the reduction of Co oxides giving the higher number of the Co metal surface atoms for catalyzing the reaction. Thus, 20-Co/ZrB-1 exhibited the highest activity. Considering the product selectivity upon methanation condition as seen in **Table 5.6**, it was found that the selectivity to C_2-C_4 products dramatically decreased with increasing the amounts of Co loading on the zirconia supports.

Table 5.6 Results of H_2 chemisorption, steady-state rate and selectivity to products

Catalyst Sample	**Total H_2 chemisorption (µmol/g cat)**	**Steady-state Rate[a] (x10^2gCH_2/gcat.h)**	**CH_4 Selectivity (%)**	**C_2-C_4 Selectivity (%)**
5-Co/ZrB-1	0.04	0.04	89.2	10.8
10-Co/ZrB-1	0.06	0.98	96.0	4.0
15-Co/ZrB-1	0.12	2.19	93.4	6.6
20-Co/ZrB-1	0.47	25.23	99.0	1

[a] CO hydrogenation was carried out at 220^{o}C, 1 atm and H_2/CO/Ar = 20/2/8. The steady-state was reached after 5 h.

CHAPTER VI

CONCLUSIONS AND RECOMMENDATION

This chapter is focused upon the conclusions of the experimental details of cobalt (Co) catalysts dispersed on various boron modified zirconia for carbon monoxide (CO) hydrogenation reaction which were described in section 6.1. In addition, recommendations for further study are given in section 6.2.

6.1 Conclusions

6.1.1 Various boron loading of 20 wt% cobalt on boron modified zirconia supported catalyst.

It appeared that B modification on the zirconia supports resulted in increased activities based on CO hydrogenation without a dramatic change in the product selectivity. The increased activities can be attributed to higher dispersion of Co oxide species on the support. It was suggested that the role of B modification could be drawn based on (i) preventing the agglomeration of Co oxide species and (ii) increasing the dispersion of the Co oxide species, then facilitating reduction of Co oxides to Co metal surface atoms for catalyzing the reaction.

6.1.2 Various Co loading of 1 wt% boron modified zirconia supported catalyst.

Based on the study, the support interaction and particle size, the nature of supports used was also the key to determine the number of active sites present. For the zirconia support, higher cobalt dispersed on zirconia was more active. There was no significant change in morphologies and elemental distributions of samples as seen from SEM/EDX. The small amount of cobalt in the boron modified zirconia supports could result in the small amount of active Co metal atoms as detected using H_2 chemisorption due to the strong support interaction. This resulted in decreasing

activity of the sample. Thus, 20-Co/ZrB-1 exhibited the highest activity.The selectivity to C2-C4 dramatically increased with decreased Co loading.

6.2 Recommendations

1. In order to investigate on different interactions, difference kinds of zirconia supports should be applied to use for boron modification.

2. Besides Co metal, other metals such as Ni, Pd, Fe and etc should be further investigated with the boron-modifed zirconia supports.

REFERENCES

Brik, Y., Kacimi, M., Verduraz, F.B., Ziyad, M. Characterization and Comparison of the Activity of Boron-Modified Co/TiO_2 Catalysts in Butan-2-ol Conversion and Oxidative Dehydrogenation of Ethane. J. Catal. 211(2002): 470-481.

Coville, N.J. and Li, J. Effect of boron source on the catalyst reducibility and Fischer–Tropsch synthesis activity of Co/TiO2 catalysts. Catal. Today 71(2002), 403-410.

Enache, D. I.; et al. Differences in the Characteristics and the Catalytic Properties of cobalt based Fischer-Tropsch catalysts supported on zirconia and alumina. Appl. Catal. A: General 268(2004): 51-56.

Farrauto, R.J. and Bartholomew, C.H. Fundamentals of indrustrial catalytic processes.1 st ed. London: Chapman & Hall, 1997.

Heuer, A.H. Transformation Toughening in ZrO_2-containing Ceramics. J. Am. Ceram. Soc. 70(1987): 689-698.

Jacobs, G., Das, T., Zhang, Y.Q., Li, J.L., Racoillet, G., Davis, B.H. Fischer–Tropsch synthesis: support, loading, and promoter effects on the reducibility of cobalt catalysts. Appl. Catal. A. 233 (2002): 263-281.

Jacobs, G., Patterson, P.M., Zhang, Y.Q., Das, T., Li, J.L., and Davis, B.H. Fischer–Tropsch synthesis: deactivation of noble metal-promoted Co/Al_2O_3 catalysts. Appl. Catal. A. 233 (2002): 215-266.

Jongsomjit, B., and Goodwin, Jr., J.G. Co-support compound formation in Co/Al_2O_3 catalysts: effect of reduction gas containing CO. Catal. Today 77 (2002): 191-204.

Jongsomjit, B., Panpranot, J., and Goodwin, Jr., J.G. Co-Support Compound Formation in Alumina-Supported Cobalt Catalysts. J. Catal. 204 (2001): 98-109.

Jongsomjit, B., Panpranot, J., and Goodwin, Jr., J.G. Effect of zirconia-modified alumina on the properties of Co/γ -Al_2O_3 catalysts. J. Catal. 215 (2003): 66-77.

Jongsomjit, B., Sakdamnuson, C, and Goodwin, Jr., J.G.,and Praserthdam, P. Co-Support Compound Formation in Titania-Supported Cobalt Catalyst. Catal. Lett. 94 (2004): 209-215.

Jongsomjit, B., Sakdamnuson, C., Praserthdam, P. Dependence of crystalline phases in titania on catalytic properties during CO hydrogenation of Co/TiO_2 catalysts. Mater. Chem. Phys. 89 (2005): 395-401.

Jongsomjit, B., Wongsalee, T., and Praserthdam, P. Study of cobalt dispersion on titania consisting various rutile: anatase ratios. Mater. Chem. Phys. 92 (2005): 572-577.

Jongsomjit, B., Wongsalee, T., and Praserthdam, P. Characteristics and catalytic properties of Co/TiO_2 for various rutile: anatase ratios. Catal. Comm. 6 (2005): 705-710.

Klug, H.P., Alexander, L.E. X-ray diffraction procedures for polycrystalline amorphous, 2 ed., Wiley, New York, 1974.

Kogelbauer, A., Weber, J.C., and Goodwin, J.G., Jr. The formation of cobalt silicates on Co/SiO_2 under hydrothermal condition. Catal Lett. 34 (1995): 259-267.

Kraum, M., and Baerns, M. Fischer-Tropsch synthesis: the influence of various cobaltcompounds applied in the preparation of supported cobalt catalysts on their performance. Appl. Catal. A 186 (2002): 189-200.

Li, J. and Coville, N.J. The effect of boron on the catalyst reducibility and activity of Co/TiO2 Fischer Tropsch catalysts. Appl. Catal. A.:General 181 (1999): 201-208.

Li, J. and Coville, N.J. Effect of boron on the sulfur poisoning on Co/TiO2 Fischer–Tropsch catalysts. Appl. Catal. A.:General 208 (2001): 177-184.

Li, J., Jacobs, G., Zhang, Y., Das, T., Davis, B.H. Fischer–Tropsch synthesis: effect of small amounts of boron, ruthenium and rhenium on Co/TiO2 catalysts. Appl. Catal. A. 223 (2002): 195-203.

Livage, J.; Doi, K.; and Mazieres, C. Nature and thermal evolution of amorphous hydrated zirconium oxide. J. Am. Ceram. Soc. 51(1968): 349-353.

Madikizela, N.N., and Coville, N.J. A study of $Co/Zn/TiO_2$ catalysts in the fischer-tropsch reaction. J. Mol. Catal. A 181 (2002): 129-136.

Othmer, K. Encyclopedia of chemical technology. Vol. 6. 4 th ed. New York: A Wiley Interscience Publication, John Wiley&Son, 1991.

Osendi, M. I.; et al. Metastability of tetragonal zirconia powders. J. Am. Ceram. Soc. 68(1985): 135-139.

Panpranot, J., Taochaiyaphum, N., and Praserthdam, P. Glycothermal synthesis of nanocrystalline zirconia and their applications as cobalt catalyst supports. Mater. Chem. Phys. 94 (2005): 207-212.

Panpranot, J., Taochaiyaphum, N., Jongsomjit, B., and Praserthdam,P. Differences in characteristics and catalytic properties of Co catalysts supported on micron- and nano-sized zirconia. Catal. Comm. 7 (2006) 192-197.

Reuel, R.C., and Bartholomew, C.H. The stoichiometries of H_2 and CO adsorption on cobalt: effects of support and preparation. J. Catal. 82 (1984): 63-77.

Schanke, D., Vada, S., Blekkan, E.A., Hilmen, A., Hoff, A., Holmen, A. J. Catal. 156 (1995): 85.

Soisuwan, P., Praserthdam, P., Panpranot , J., Trimm, D.L. Effect of Si- and Y-modified nanocrystalline zirconia on the properties of Co/ZrO_2 catalysts. Catal.Comm. 7(2006) 761.

Stranick, M.A.; Houalla, M.; Hercules, D.M. The Effect of Boron on the State and Dispersion of Co/Al2O3 Catalysts. J. Catal. 104 (1987): 396-412.

Tani, E.; Yoshimura, M.; and Somiya, S. Formation of Ultrafine tetranol ZrO_2 powder under hydrothermal conditions. J. Am. Ceram. Soc. 66(1982): 11-14.

West, A.R.; Solid State Chemistry and its Application, John Wiley&Sons, Brisbane, 1997.

Wongsalee, T., Jongsomjit, B., Praserthdam, P. Effect of zirconia-modified titania consisting of different phases on characteristics and catalytic properties of Co/TiO_2 catalysts Catal. Lett. 108 (2006): 55-61.

Young, R.S. COBALT: Its Chemistry, Metallurgy, and Uses. New York: Reinhpld Publishing Corporation, 1960.

Zhang, Y., Wei, D., Hammache, S., Goodwin Jr., J.G. Effect of water vapor on the reduction of Ru-promoted Co/Al_2O_3**.** J. Catal. 188 (1999): 281-290.

APPENDICES

APPENDIX A

CALCULATION FOR CATALYST PREPARATION

Preparation of 20%Co/SiO_2-ZrO_2 catalysts by the incipient wetness impregnation method are shown as follows.

Reagent: - Cobalt (II) nitrate hexahydrate [$Co(NO_3)_2 \cdot 6H_2O$]

Molecular weight = 291.03 g

- Nano-SiO_2 support
- Nano-ZrO_2 support
- Micron-SiO_2 support
- Micron-ZrO_2 support

Example calculation for the preparation of 20%Co/Si-0-Zr-100

Based on 100 g for catalyst used, the composition of the catalyst will be as follows:

Cobalt = 20 g

ZrO_2 = 100-20 = 80 g

For 5 g of catalyst

Cobalt required = $1 \times (20/80)$ = 0.2 g

Cobalt 0.2 g was prepared from $Co(NO_3)_2 \cdot 6H_2O$ and molecular weight of Co is 58.93

$$Co(NO_3)_2 \cdot 6H_2O \text{ required} = \frac{MW\ of\ Co(NO_3)_2 \cdot 6H_2O \times cobalt\ required}{MW\ of\ Co}$$

$$= (291.03/58.93) \times 0.2 = 0.99 \text{ g}$$

Since the pore volume of the pure zirconia support is 0.402 ml/g for ZrO_2. Thus, the total volume of impregnation solution which must be used is 0.803 ml for ZrO_2 by the requirement of incipient wetness impregnation method, the de-ionized water is added until equal pore volume for dissolve Cobalt (II) nitrate hexahydrate.

APPENDIX B

CALCULATION FOR TOTAL H_2 CHEMISSORPTION AND DISPERSION

Calcution of the total H_2 chemisorption and metal dispersion of the catalyst, a stoichiometry of H/Co = 1, measured by H_2 chemisorption is as follows:

Let the weight of catalyst used	=	W	g
Integral area of H_2 peak after adsorption	=	A	unit
Integral area of 45 µl of standard H_2 peak	=	B	unit
Amounts of H_2 adsorbed on catalyst	=	B-A	unit
Concentration of Co (by AAS)	=	C	%wt
Volume of H_2 adsorbed on catalyst	=	$45 \times [(B - A) / B]$	µl
Volume of 1 mole of H_2 at 100°C	=	28.038	µl
Mole of H_2 adsorbed on catalyst	=	$[(B - A) / B] \times [45 / 28.038]$	µmole

Total H_2 chemisorption $= [(B - A) / B] \times [45 / 28.038] \times [1 / W]$ µmole/g of catalyst

$= N$ µmole/g of catalyst

Molecular weight of cobalt = 58.93

Metal dispersion (%) $= \dfrac{2 \times H_{2\,tot} / g\ of\ catalyst \times 100}{No\ \mu mole\ Co_{tot} / g\ of\ catalyst}$

$= \dfrac{2 \times N \times 100}{No\ \mu mole\ Co_{tot}}$

$= \dfrac{2 \times N \times 58.93 \times 100}{C \times 10^6}$

$= \dfrac{1.179 \times N}{C}$

APPENDIX C

CALIBRATION CURVES

This appendix showed the calibration curves for calculation of composition of reactant and products in CO hydrogenation reaction. The reactant is CO and the main product is methane. The other products are linear hydrocarbons of heavier molecular weight that are C_2-C_4 such as ethane, ethylene, propane, propylene and butane.

The thermal conductivity detector, gas chromatography Shimadzu model 8A was used to analyze the concentration of CO by using Molecular sieve 5A column.

The VZ10 column are used with a gas chromatography equipped with a flame ionization detector, Shimadzu model 14B, to analyze the concentration of products including of methane, ethane, ethylene, propane, propylene and butane. Conditions uses in both GC are illustrated in Table C.1.

Mole of reagent in y-axis and area reported by gas chromatography in x-axis are exhibited in the curves. The calibration curves of CO, methane, ethane, ethylene, propane, propylene and butane are illustrated in the following figures.

Table C.1 Conditions use in Shimadzu modal GC-8A and GC-14B.

Parameters	Condition	
	Shimadzu GC-8A	Shimadzu GC-14B
Width	5	5
Slope	50	50
Drift	0	0
Min. area	10	10
T.DBL	0	0
Stop time	50	60
Atten	0	0
Speed	2	2
Method	41	41
Format	1	1
SPL.WT	100	100
IS.WT	1	1

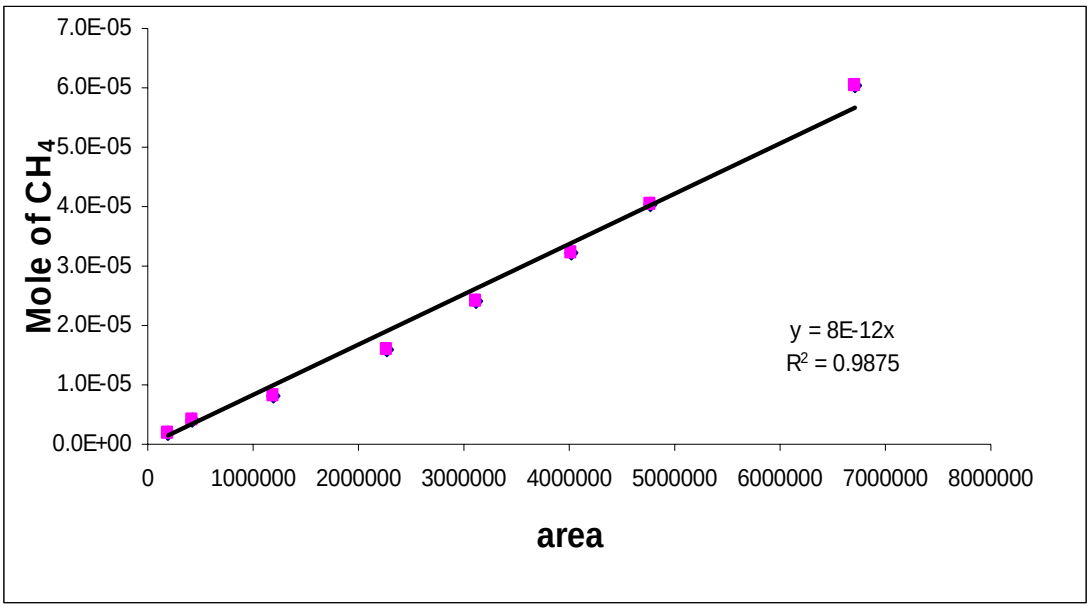

Figure C.1 The calibration curve of methane.

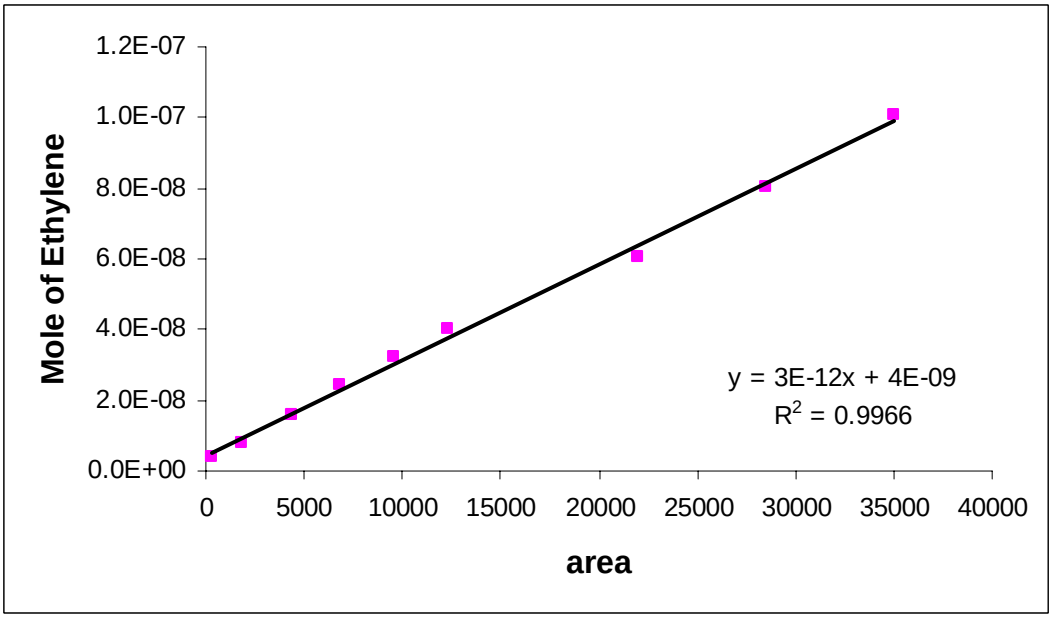

Figure C.2 The calibration curve of ethylene.

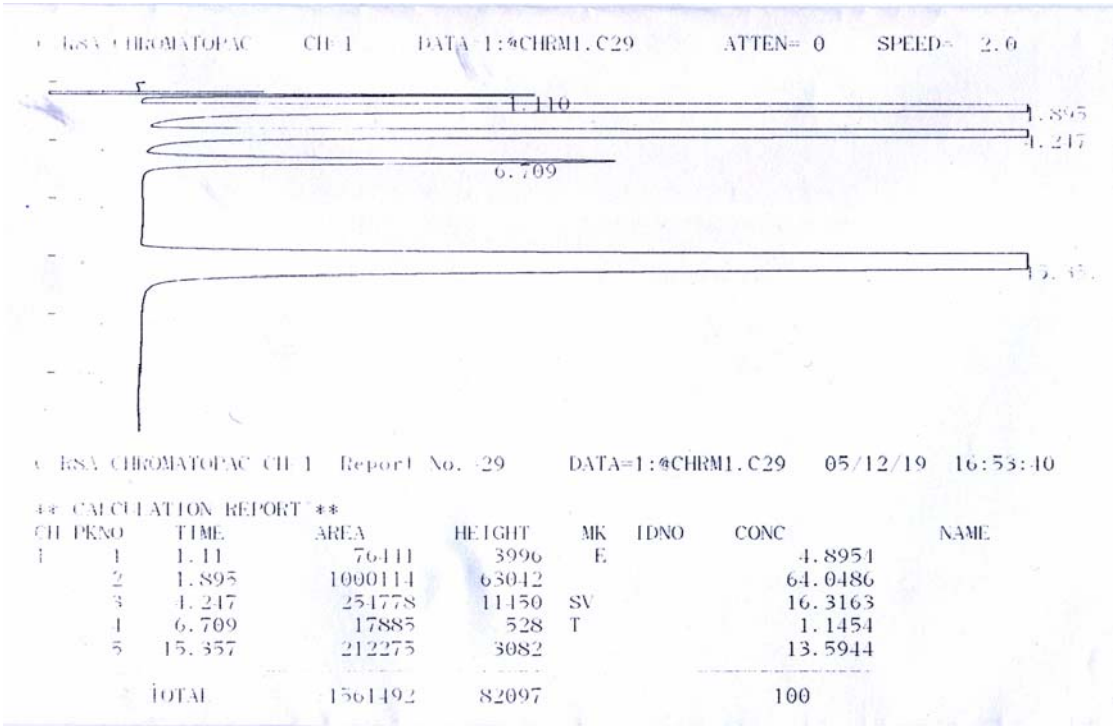

Figure C.3 The chromatograms of catalyst sample from thermal conductivity detector, gas chromatography Shimadzu model 8A (Molecular sieve 5A column).

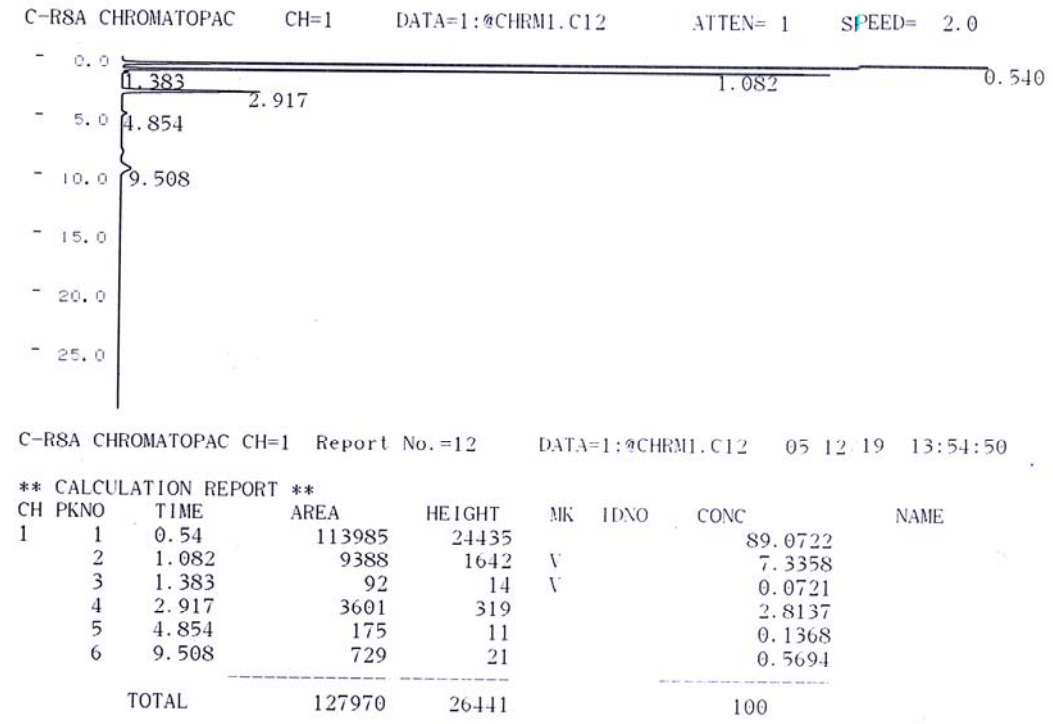

Figure C.4 The chromatograms of catalyst sample from flame ionization detector, gas chromatography Shimadzu model 14B (VZ10 column).

APPENDIX D

CALCULATION OF CO CONVERSION, REACTION RATE AND SELECTIVITY

The catalyst performance for the CO hydrogenation was evaluated in terms of activity for CO conversion rate and selectivity.

Activity of the catalyst performed in term of carbon monoxide conversion and reaction rate. Carbon monoxide conversion is defined as moles of CO converted with respect to CO in feed:

$$\text{CO conversion (\%)} = \frac{100 \times [mole\ of\ CO\ in\ feed - mole\ of\ CO\ in\ product]}{mole\ of\ CO\ in\ feed} \quad \text{(i)}$$

Reaction rate was calculated from CO conversion that is as follows:

Let the weight of catalyst used	=	W	g
Flow rate of CO	=	2	cc/min
Reaction time	=	60	min
Weight of CH_2	=	14	g
Volume of 1 mole of gas at 1 atm	=	22400	cc

$$\text{Reaction rate (g } CH_2\text{/g of catalyst)} = \frac{[\%\ conversion\ of\ CO/100] \times 60 \times 14 \times 2}{W \times 22400} \quad \text{(ii)}$$

Selectivity of product is defined as mole of product (B) formed with respect to mole of CO converted:

$$\text{Selectivity of B (\%)} = 100 \times [mole\ of\ B\ formed / mole\ of\ total\ products] \quad \text{(iii)}$$

Where B is product, mole of B can be measured employing the calibration curve of products such as methane, ethane, ethylene, propane, propylene and butane

$$\text{mole of } CH_4 = (area\ of\ CH_4\ peak\ from\ integrator\ plot\ on\ GC - 14B) \times 8 \times 10^{12} \quad \text{(iv)}$$

APPENDIX E

LIST OF PUBICATIONS

1. Nithinart Chitpong, Bunjerd Jongsomjit and Piyasan Praserthdam, "Investigation of boron-modified zirconia on characteristics and catalytic properties of Co/ZrO_2-B catalysts towards CO hydrogenation" Submitted to Catalysis Letters, 2007. (in review)
2. Nithinart Chitpong, Bunjerd Jongsomjit and Piyasan Praserthdam, " Effect of cobalt loading on Catalytic properties towards CO hydrogenation of Co/ZrO_2 with boron modification" Submitted to Materials Chemistry and Physics, 2007. (be submitted)
3. Nithinart Chitpong, Bunjerd Jongsomjit and Piyasan Praserthdam, "Effect of boron-modified zirconia-supported cobalt catalysts and their catalytic properties via CO hydrogenation", Proceeding of the Regional Symposium on Chemical Engineering 2006 Conference 13^{th} (RSCE 2006), Nanyang Technological University, Singapore, Dec., 2006, page 58.

ต้นฉบับไม่มีหน้า 64-66
NO PAGE 64-66 IN ORIGINAL

VITAE

Miss Nithinart Chitpong was born on June 16th, 1983 in Bangkok, Thailand. She finished high school from Samsenwitthayalai School, bangkok in 2001, and received the Brachelor degree of the department of chemical science from Chulalongkorn University in March 2005. She continued her Master's study at the department of Chemical Engineering, Chulalongkorn University in 2005.